UNITED STATES EXPERIMENTAL MODEL BASIN

NAVY YARD, WASHINGTON, D.C.

FORM RESISTANCE EXPERIMENTS OF 1937 AND 1938

BY C. E. JANES

RESTRICTED

CONTENTS OF THIS REPORT NOT TO BE DIVULGED OR REFERRED TO IN ANY PUBLICATION. IN THE EVENT INFORMATION DERIVED FROM THIS REPORT IS PASSED ON TO OFFICER OR CIVILIAN PERSONNEL, THE SOURCE SHOULD NOT BE REVEALED.

JULY 1940 REPORT 453

FORM RESISTANCE EXPERIMENTS OF 1937 AND 1938

by

C. E. Janes

U.S. Experimental Model Basin
Navy Yard, Washington, D.C.

July 1940 Report 453

FORM RESISTANCE EXPERIMENTS OF 1937 AND 1938

SUMMARY

In a new series of form resistance experiments on a special model with a pronounced bulb bow, the resistance of the model was determined from extensive point-pressure measurements over its surface.

It is shown that up to a high speed the form resistance so calculated is greater than the residuary resistance derived by the usual Froude method. The inference is that over this speed range the actual frictional resistance is lower than the estimated resistance.

Measurements were also made with the model self-propelled, to determine the change in form resistance caused by propeller action. It is shown that this change is only about one-half the augmented resistance. The difference must for the present be ascribed to an increase in frictional and eddy resistance created by acceleration of the water by the propellers.

INTRODUCTION

In Experimental Model Basin Report 392, "Preliminary Report on Residuary or Form Resistance of Ships," November, 1934, there were published the results of basin experiments on the special Model 2861, undertaken in an endeavor to determine form resistance by a more or less direct method. This report described and discussed the results of measurements of pressures normal to the hull at numerous points over the underwater surface of the model. The conclusion was that this method of attack offered considerable promise of arriving at a true measure of the form resistance of a ship, and that it might ultimately be more reliable than the time-honored indirect method of deducing residuary resistance by a calculation embodying doubtful frictional resistance.

EXTENSION OF PREVIOUS EXPERIMENTS

There were three reasons for extending the scope of the original form resistance experiments on Washington Model 2861 and refining the apparatus:

1. The measurement of net resistance on the separate bow and stern of this model was extremely difficult; at best the results were uncertain. Further development of the pressure orifice method was indicated, especially the use of a greater number of orifices and a better distribution over the hull. For convenience, experimental work of this kind will henceforth be referred to as the measurement of point pressures.

2. The important area in the forebody above the normal waterline, covered by the bow wave when the model was underway, and distinguished

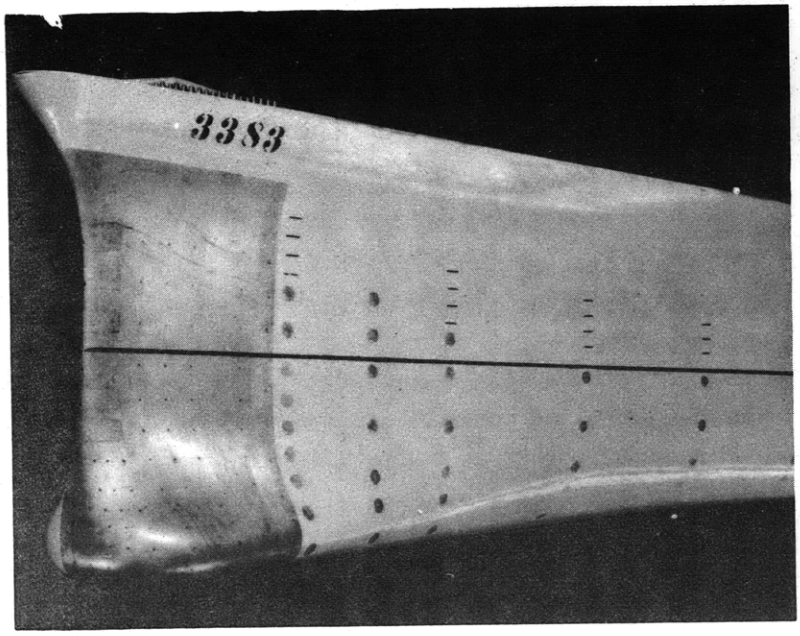

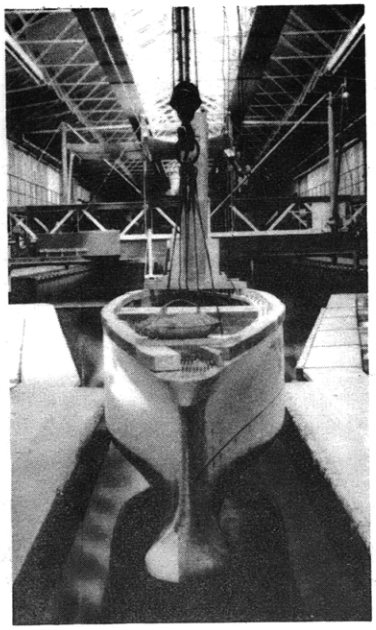

Figure 1

Figure 1a

General Views of Bow of Model 3383

The near side of the bow (Figure 1) shows the white metal casting containing closely spaced orifices. In the remaining area, the orifices are located in the centers of the large disks. The copper tubes for attachment to the manometer appear just above the number on the model.

In Figure 1a the extreme bulb bow is visible as the model appears ready for testing in the towing tank.

by the development of high positive pressures, was not fitted with orifices on Model 2861. The technique of measuring pressures at points uncovered when the model is at rest, described in Appendix 1, had not been developed at that time.

3. Because previous tests of Model 2861 had indicated that its resistance would have been considerably reduced by the use of a bulb bow and a wider, flatter stern, it was concluded that further form resistance experiments should be conducted on a model embodying those special features.

DESCRIPTION OF NEW MODEL

A second special model, 3383, was built, having the characteristics listed in Table 1. As in the case of the first model, it was considered necessary to resort to extremes to develop large pressure differences and to reduce the effect of errors of measurement. It will be noted from Figures 1 and 1a, and from the various body plans that the model has an extreme bulb bow. Its resistance was unusually low as compared with the standard series (see Figure 4).

TABLE 1

Model 3383

Length between perpendiculars	20 feet
Beam, extreme	3.21 feet
Draft	0.96 feet
Displacement	2257 pounds
Wetted surface	72.70 square feet
Parallel middle body	none
Prismatic coefficient	0.600
Block coefficient	0.588
Waterline coefficient	0.67
Intercept of sectional area curve at FP, percentage of midship (maximum section) area	15 per cent
Tangent of sectional area curve at FP	zero

There were 40 stations, spaced 6 inches apart, between the forward and after perpendiculars. The maximum section was abaft amidships, at Station 22.

The model was equipped for self-propulsion to permit a study of thrust deduction and to show the effect of the propellers (Table 2) upon the general distribution of pressure over the hull.

TABLE 2

Model Propellers (2), Numbers 1415 and 1416

Direction of rotation	outward
Diameter	6.76 inches
Pitch	6.72 inches
Number of blades	3
Pitch/diameter ratio	0.994
Mean width ratio	0.4605
Blade thickness fraction	0.0518
Projected area/disc area ratio	0.633
Submergence of tips below surface	0.69 diameter
Appendages	rudder and bossings
Trim	zero

NUMBER AND DISTRIBUTION OF ORIFICES

There were 299 orifices for measuring point pressures. Of these, 154 were forward of Station 4, within a tenth of the length from the forward perpendicular. Of the latter group, 28 were located above the normal waterline for a study of the pressures behind the bow wave. Twenty-five special orifices were included for a

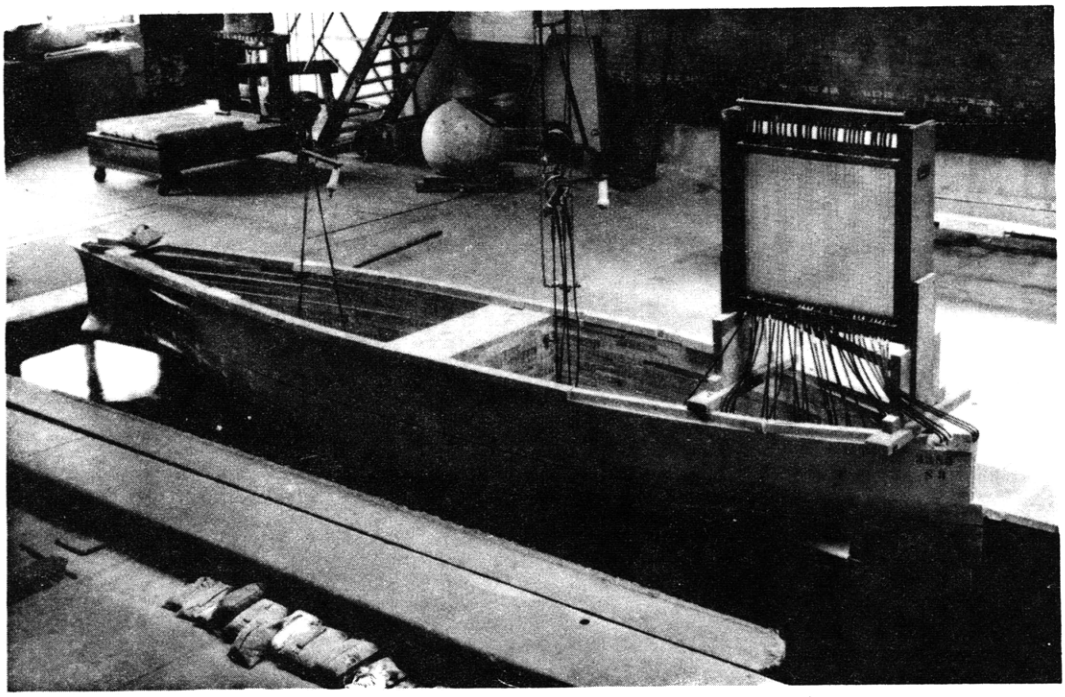

Figure 2 – Model Rigged for Pressure Tests

The glass manometer tubes are connected by rubber tubes and copper tubes to the orifices at the stern of the model.

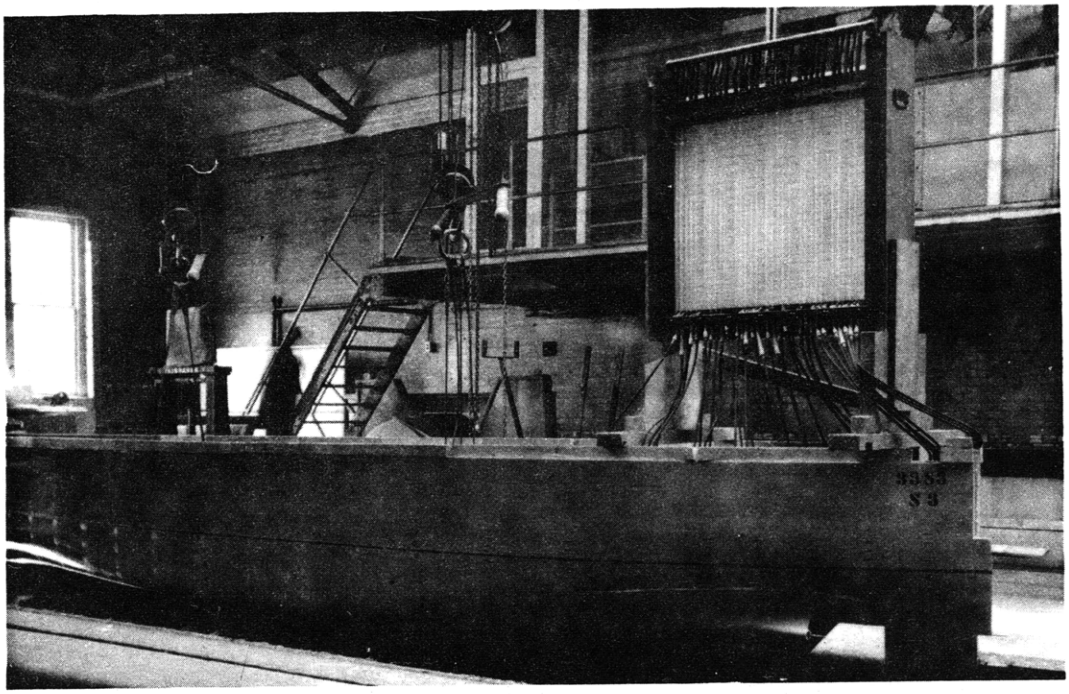

Figure 3 – Multiple-Tube Manometer for Point-Pressure Experiments

The rubber tubes indicate the positions of the glass manometer tubes, which do not show clearly in the photograph. Behind the glass tubes is a screen ruled with horizontal reference lines. Note that the bank of manometer tubes is mounted on the model and not on the carriage.

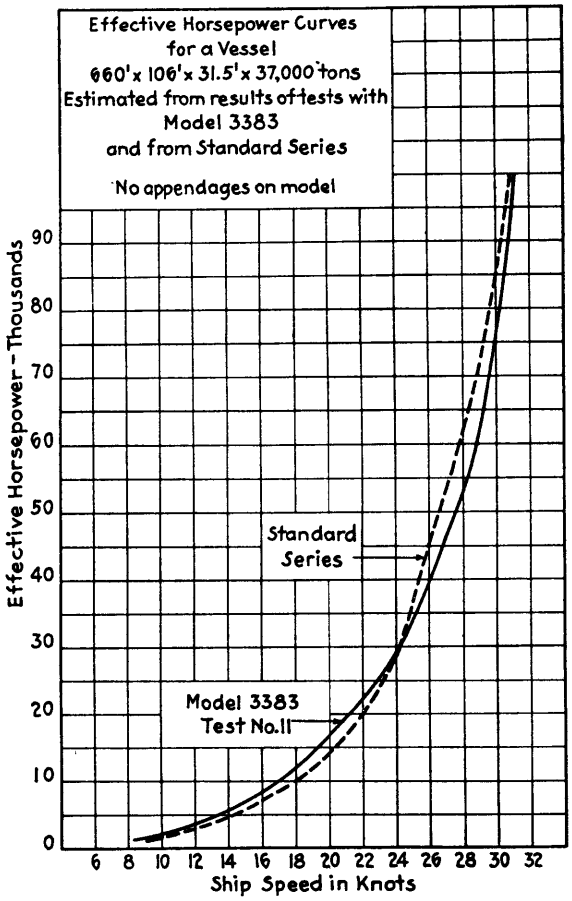

Figure 4 – Effective Horsepower Curves for Model 3383

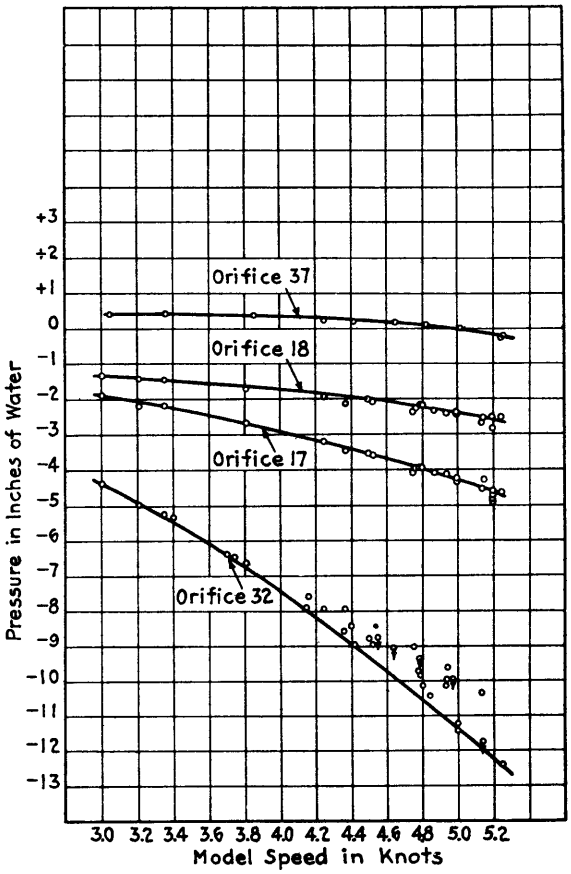

Figure 5 – Curves of Water Pressure Plotted on Model Speed

At the higher model speeds it was necessary to make several runs and to close the rubber tubes temporarily between runs so that at constant model speed there would be sufficient time for the water to balance itself in the manometer tubes before the photographic readings were taken. The spots above the curve for Orifice 32 show that this balance had not yet been reached; the spots with arrows show that the water was observed to be still moving in the tubes when the photograph was taken.

study of point pressures as affected by the working of the propellers. The exact positions of the orifices are shown on the various body plans.

The orifices, all on the port side of the model, were in general located at the transverse stations and along the waterlines, to facilitate the fairing of the curves of observed pressure. A description of the orifices, the manometers, and other details of the test apparatus will be found in Appendix 1.

TEST PROCEDURE

The manometer on the model (Figures 2 and 3) was connected to groups of orifice tubes in relays of 30. Sixteen such groups were tested, so that the pressure at nearly every orifice was measured at least twice throughout the range of

speed. Model speeds varied from 3.0 to 5.2 knots (Figure 5). There were 4,652 readings made during the towing tests alone.

The readings were recorded by photographs of the manometer. An exposure was made immediately before each run, for zero speed, and another during the run, when the water levels in the manometer tubes ceased to rise and were steady.

If the pressure at an orifice was such that the water level in the corresponding tube did not have time to come to rest during the run, the water in that tube was worked up or down by hand to the approximate position of equilibrium. The rubber tube was then clamped shut with a pinch cock until the model reached its predetermined speed, when the clamp was released and the water assumed its proper level.

The measurement of pressure at the orifices above the load waterline was based on a phenomenon observed during previous tests. It had been found that if an orifice was exposed to the air when the height of the water column above it balanced the partial vacuum in the tank on the carriage, surface tension would seal the orifice and no air would enter the tube, nor would the water run out. The mechanism developed to take advantage of this fact, together with the method of operating it, is described and illustrated in Appendix 1.

METHOD OF WORKING UP OBSERVED DATA

The change of pressure at each orifice, as indicated by the difference between the level at rest and the level at any speed, was first plotted for the range of speeds and then faired. A typical example is shown in Figure 5.

The girth of each transverse section in which orifices were located was then laid down in its expanded length, beginning from the keel at the centerline plane. On this expanded girth there was marked, in its correct position, each orifice, the waterline at rest, and the waterline (wave profile) underway.

The wave profile was marked on the surface of the model at each of the seven speeds selected for the tests. Draft marks on the model at each station in way of the wave profile allowed measurements to be made from photographs, as a check on the marked profiles.

A separate girth expansion was required for each speed, upon which the faired pressures for that speed were plotted. A curve faired through the spots thus plotted represented the variation in pressure around the section at given speed, as illustrated by Figure 6. These curves, on sections through the bulb, illustrate the high pressures and steep pressure gradients encountered in that vicinity. It is to be noted also that the curve of pressure change above the load waterline is decidedly hollow. Since the sides of the model in that region are vertical, this means that the pressure on the area covered by the part of the bow wave above the load waterline is always less than the height of the wave would indicate.

The observed pressure values for each speed were similarly plotted and faired along the waterlines, which were treated as girths. The final corrected

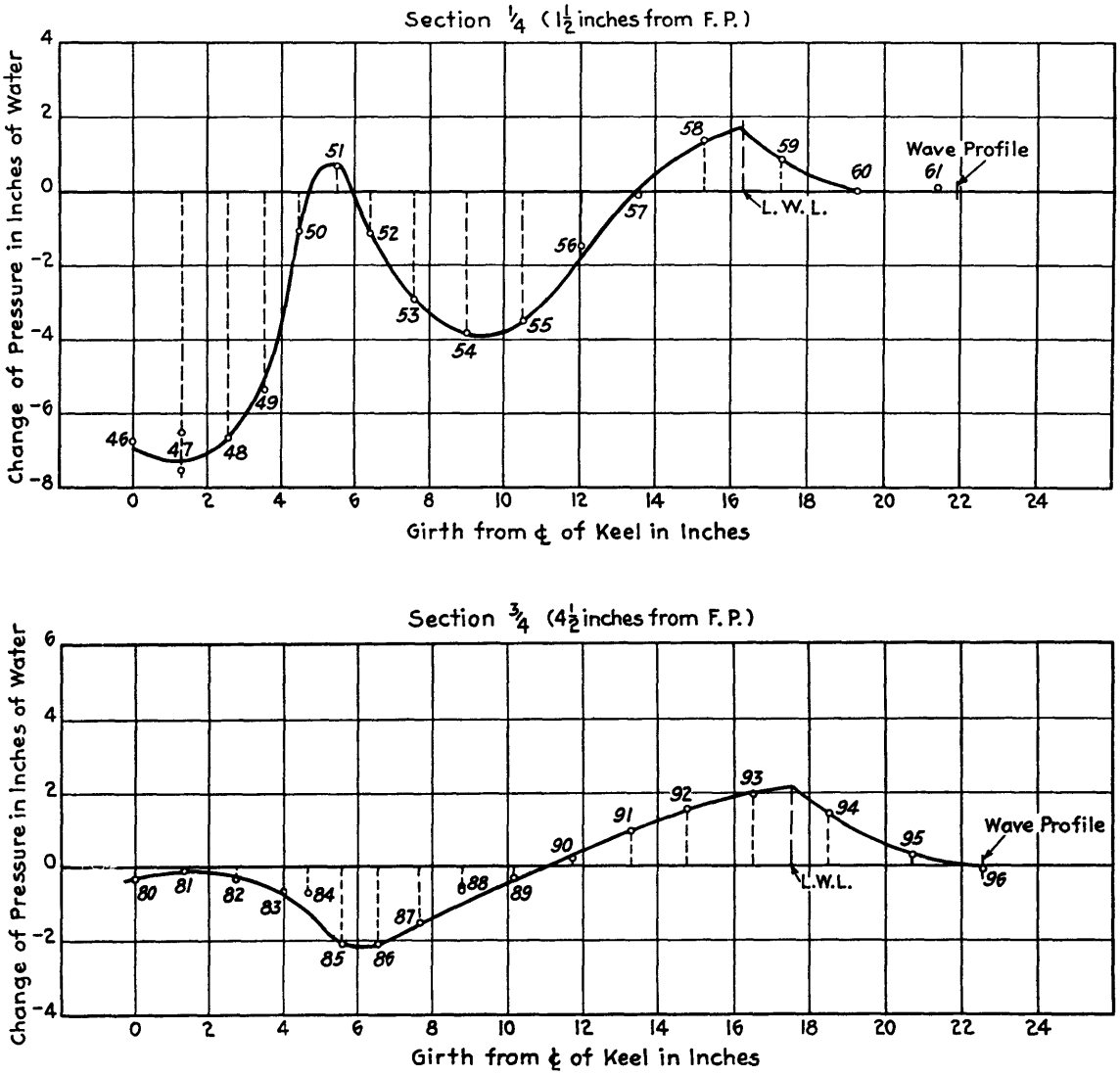

Figure 6 – Curves of Water Pressure Plotted on Girth of Sections

The spots shown are from curves of water pressure plotted on model speed (similar to the curves of Figure 5) at a model speed of 3.8 knots, before any cross fairing was done.

values of pressure for each orifice were such that fair curves could be drawn through them, whether they had been plotted on a base of speed, girth, or waterline.

These faired values of pressure for each speed were then transferred at their proper orifice positions to the body plan of the model, and contours of equal pressure were drawn, as shown in Figures 7 to 34, inclusive. Because of the peculiar form of the bulb bow, which swells out wider than some of the sections abaft it, the bow below Waterline VI and forward of Station 4 is shown on two sets of charts. Those in Figures 7 to 13 inclusive depict pressure changes on the forward side of the bulb from the forward perpendicular to Station 3/4; Figures 14 to 20 inclusive, show

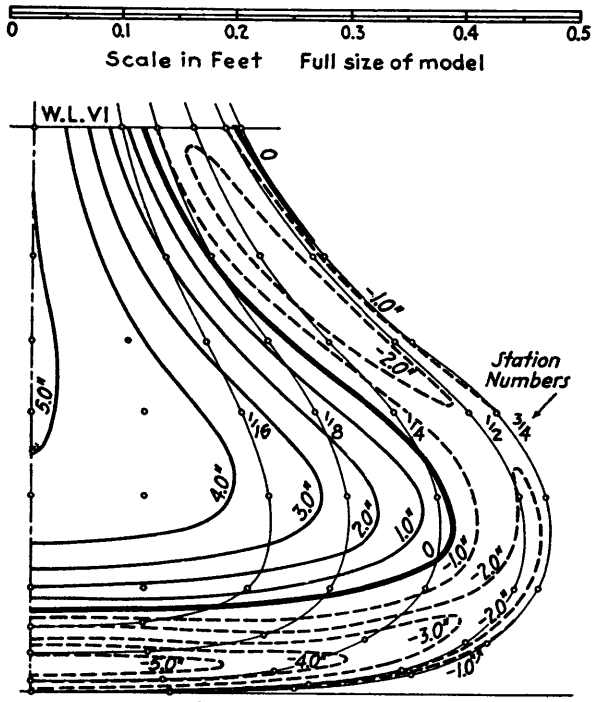

Speed=3.0 Knots

Figure 7

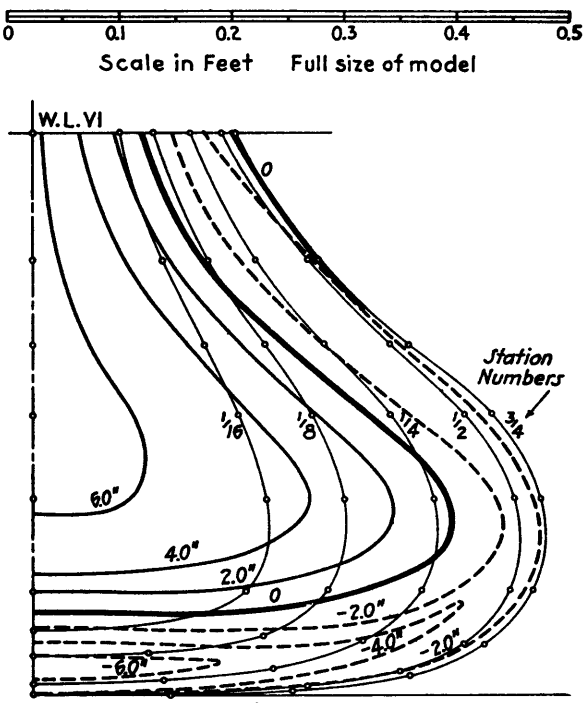

Speed=3.4 Knots

Figure 8

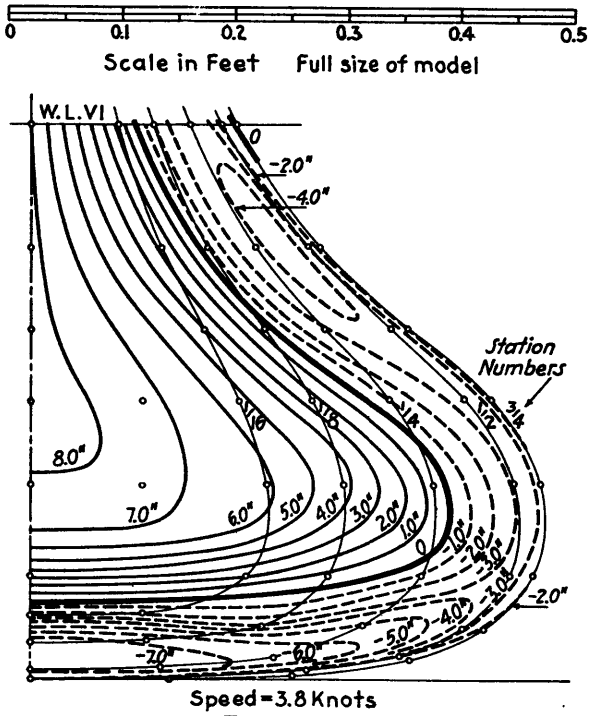

Speed=3.8 Knots

Figure 9

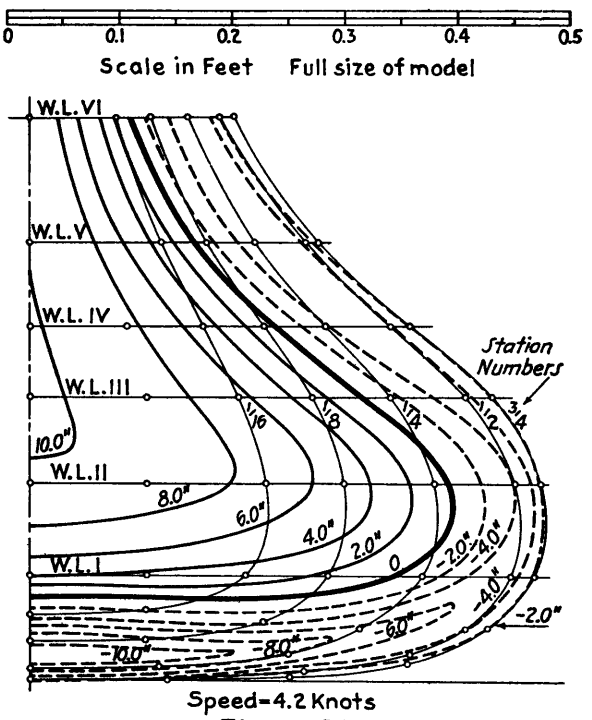

Speed=4.2 Knots

Figure 10

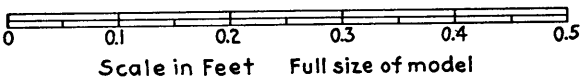

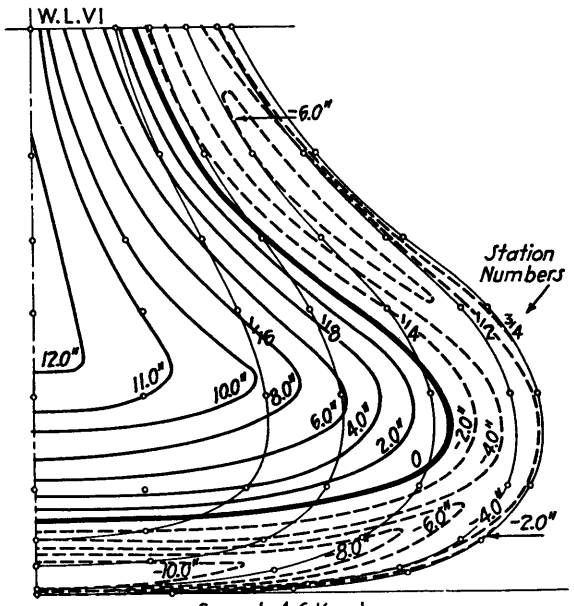

Speed=4.6 Knots

Figure 11

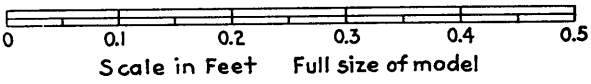

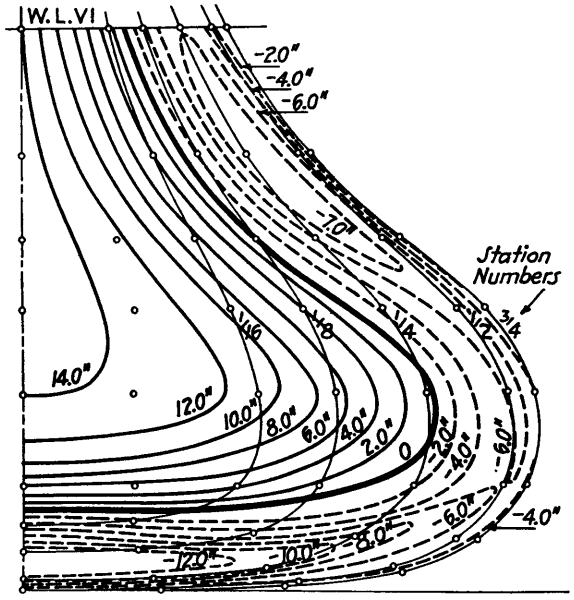

Speed=5.0 Knots

Figure 12

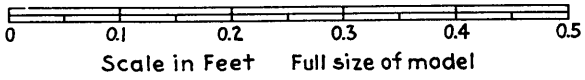

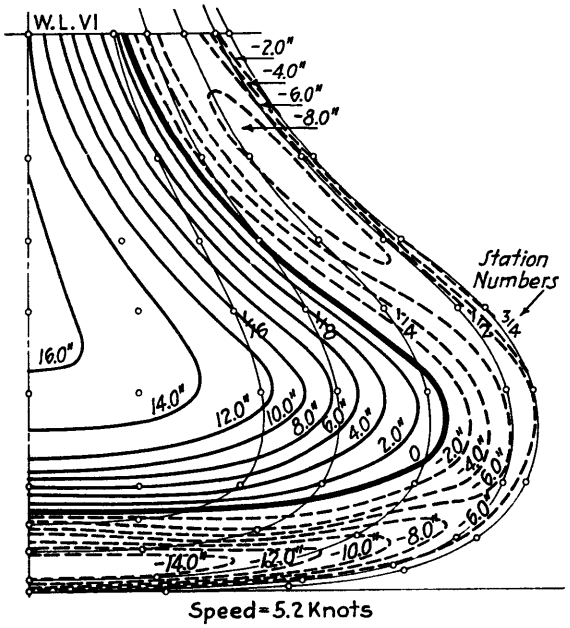

Speed=5.2 Knots

Figure 13

Contours of Change of Pressure on Lower Forward Portion of Bulb, Below the 6-inch Waterline

Half body plans of Model 3383, showing contours of change of pressure occurring from the position at rest to various model speeds. Positive pressures indicate an increase in pressure above that existing in the static condition. Small circles indicate the positions of the orifices. All pressures are expressed in inches of water.

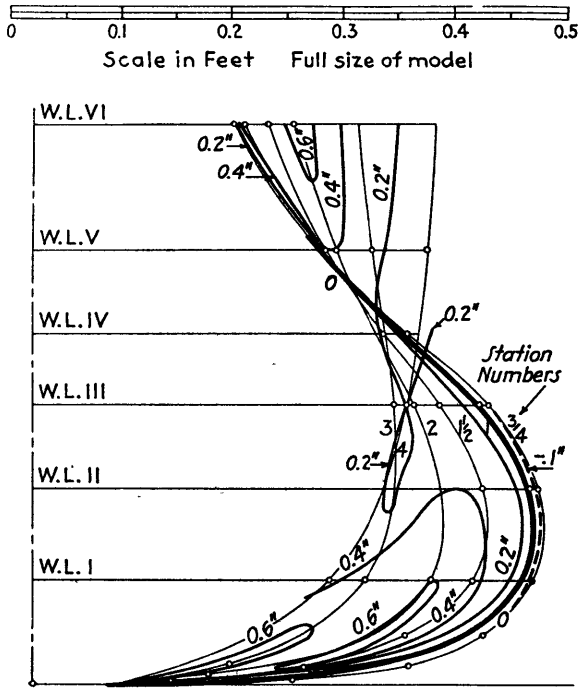

Speed=3.0 Knots

Figure 14

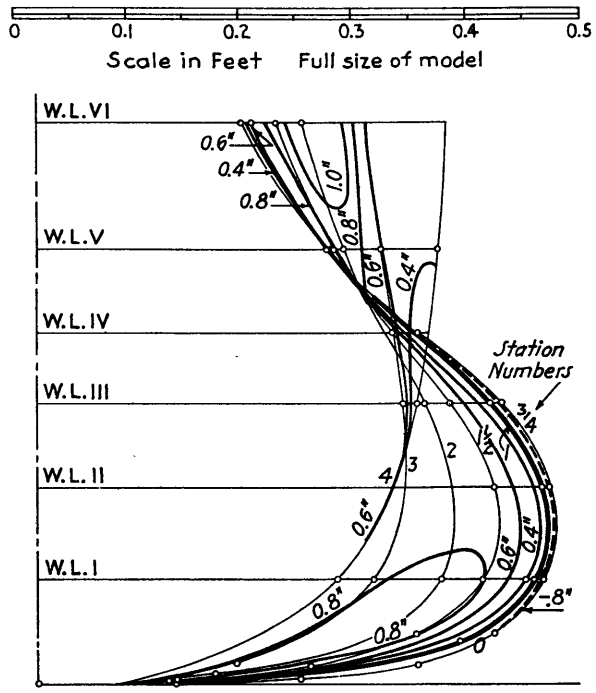

Speed=3.4 Knots

Figure 15

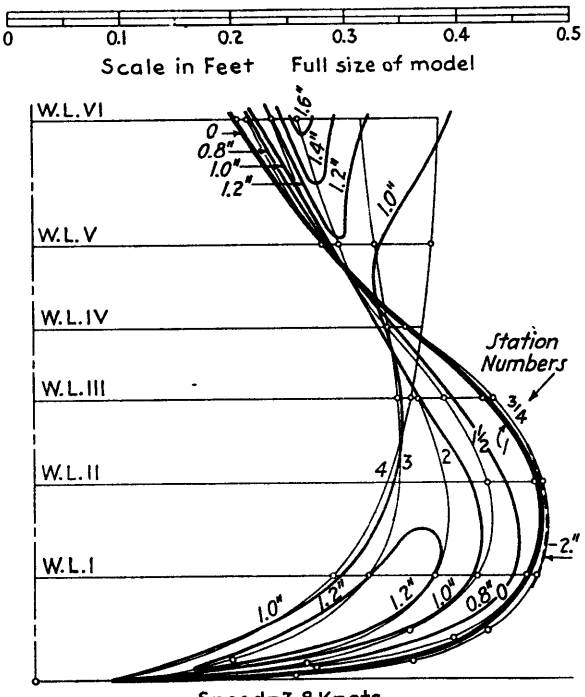

Speed=3.8 Knots

Figure 16

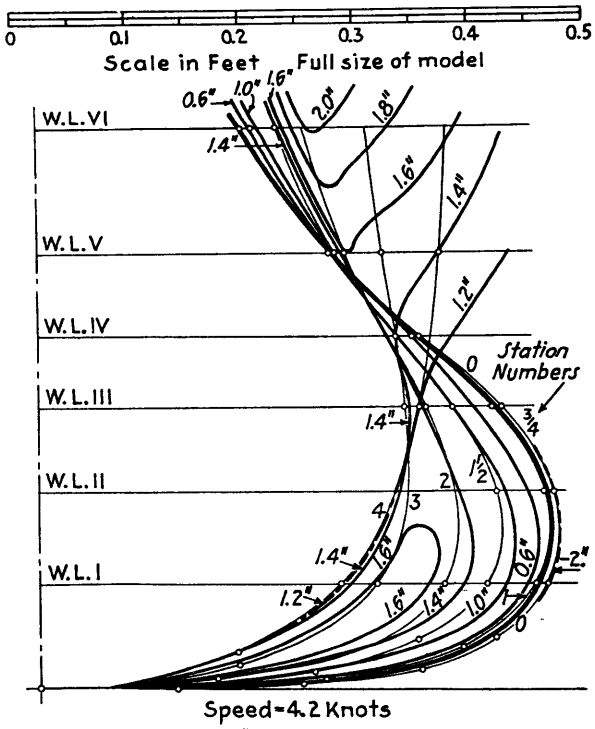

Speed=4.2 Knots

Figure 17

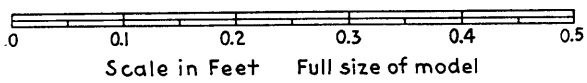

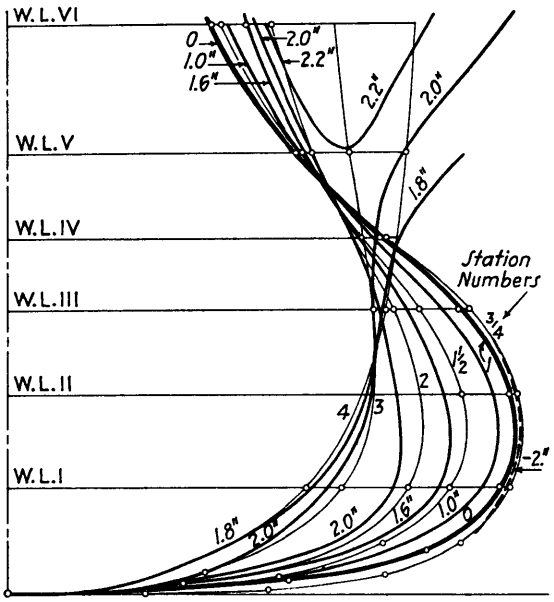

Speed-4.6 Knots

Figure 18

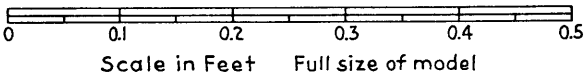

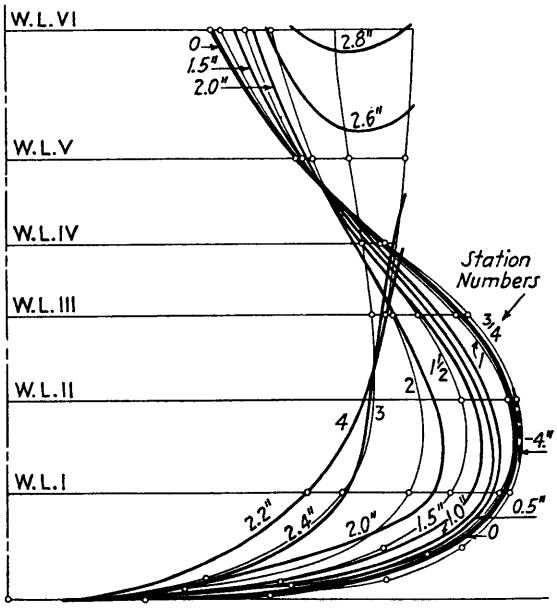

Speed-5.0 Knots

Figure 19

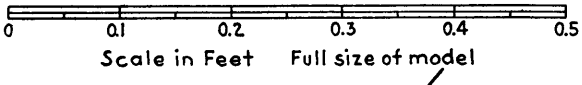

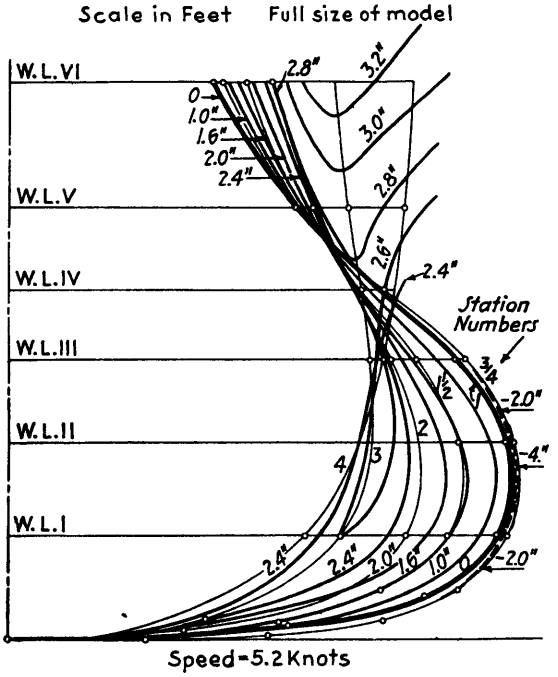

Speed-5.2 Knots

Figure 20

Contours of Change of Pressure on Lower After Portion of Bulb, Below the 6-inch Waterline

Half body plans of Model 3383, showing contours of change of pressure occurring from the position at rest to various model speeds. Positive pressures indicate an increase in pressure above that existing in the static condition. Small circles indicate the positions of the orifices. All pressures are expressed in inches of water.

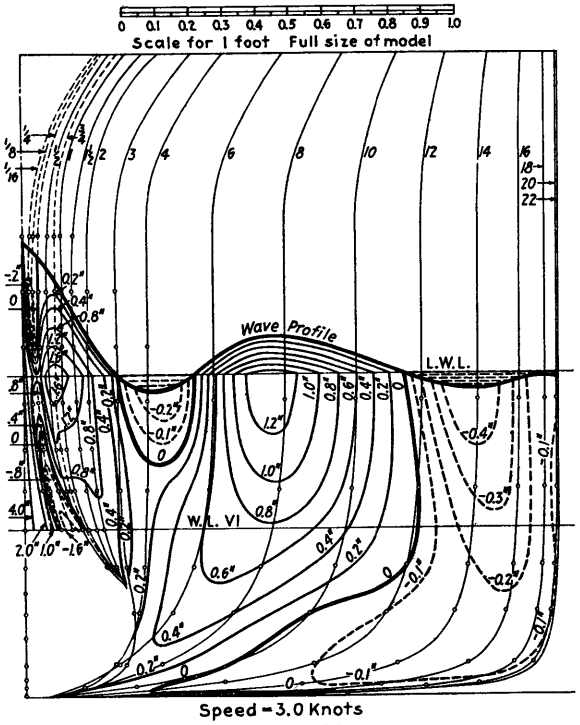

Speed = 3.0 Knots

Figure 21

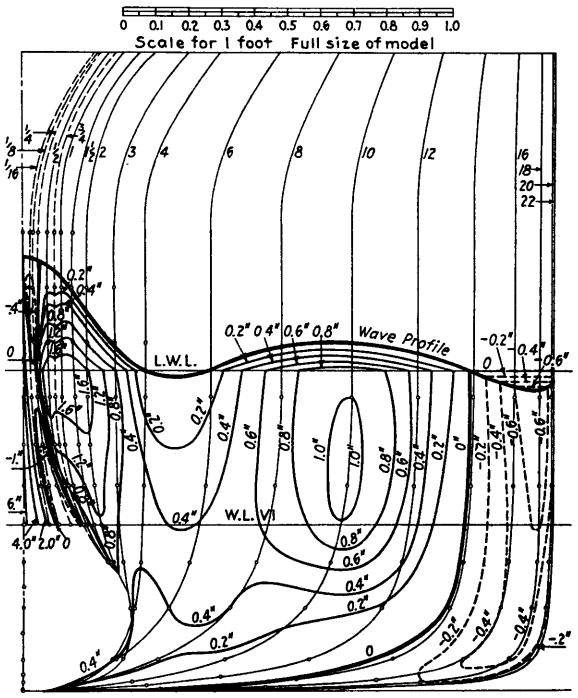

Speed = 3.4 Knots

Figure 22

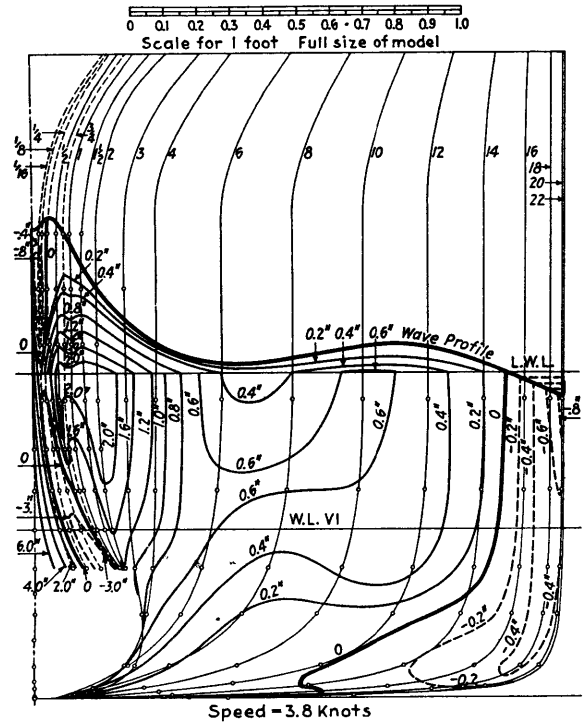

Speed = 3.8 Knots

Figure 23

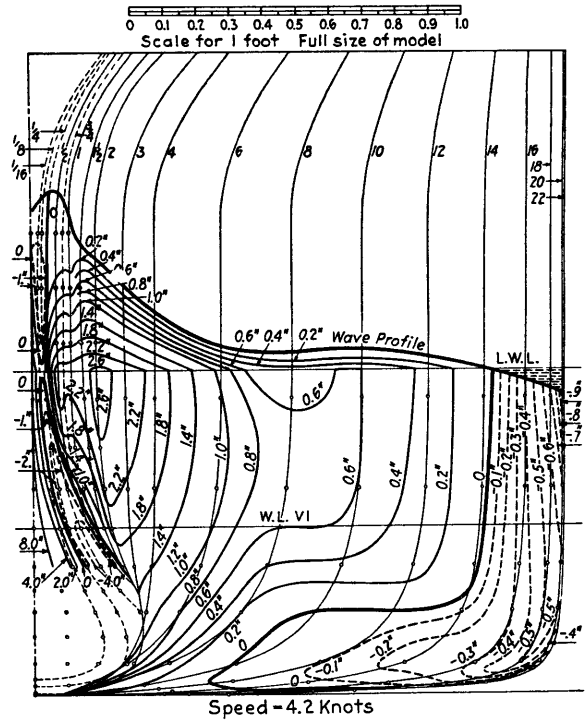

Speed = 4.2 Knots

Figure 24

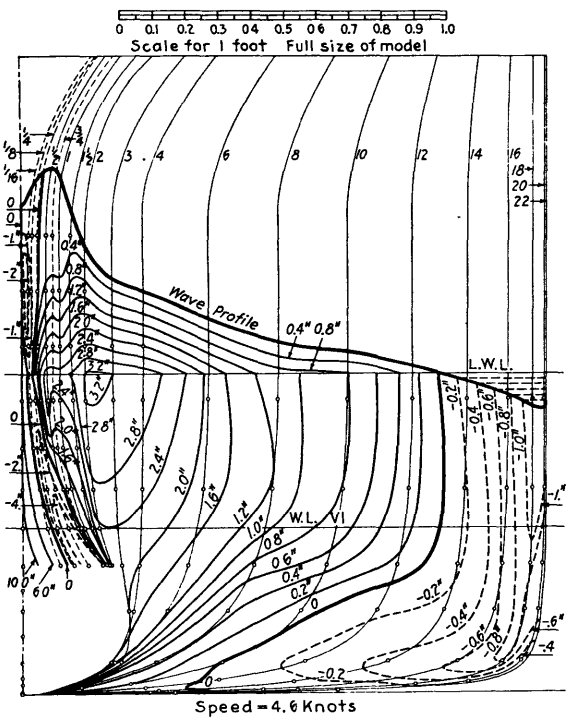

Figure 25

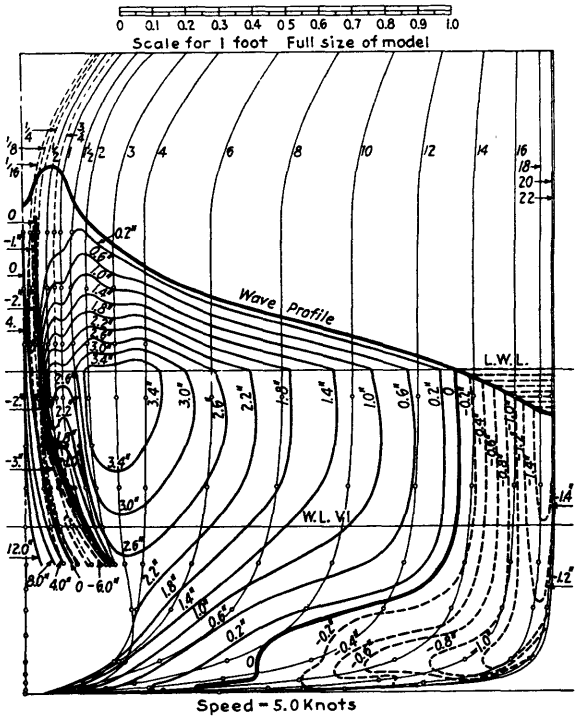

Figure 26

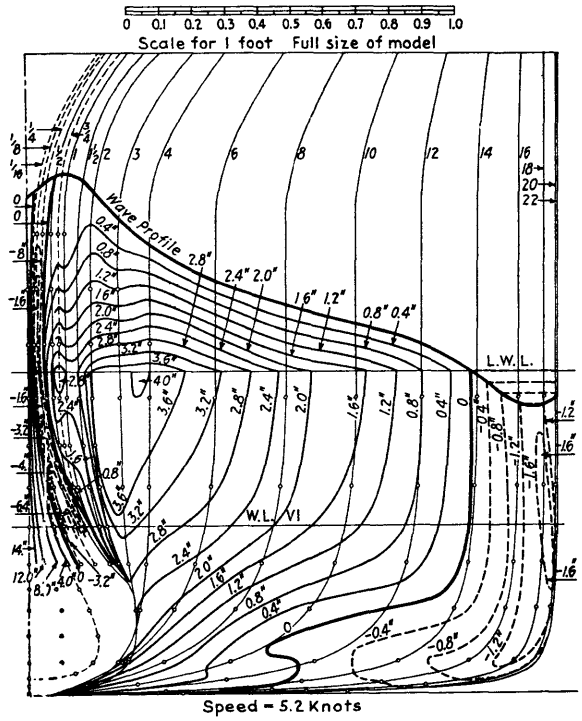

Figure 27

Contours of Change of Pressure on Forebody Excluding Bulb

Half body plans of Model 3383, showing contours of change of pressure occurring from the position at rest to various model speeds. Positive pressures indicate an increase in pressure above that existing in the static condition. Small circles indicate the positions of the orifices. All pressures are expressed in inches of water.

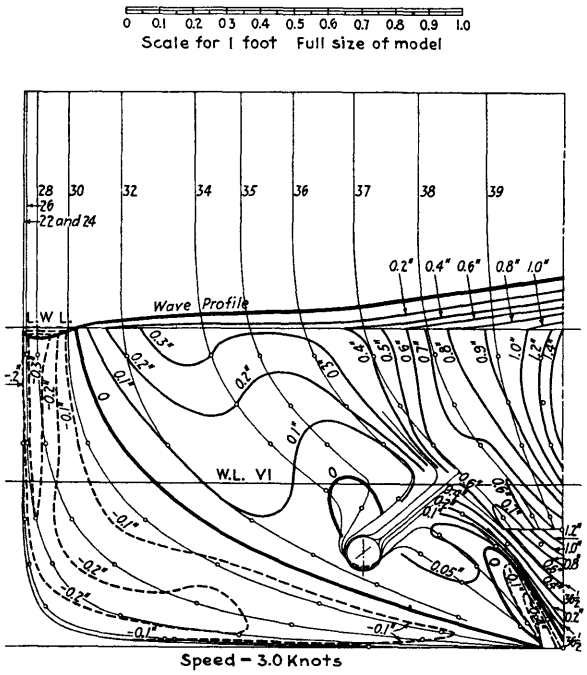

Figure 28

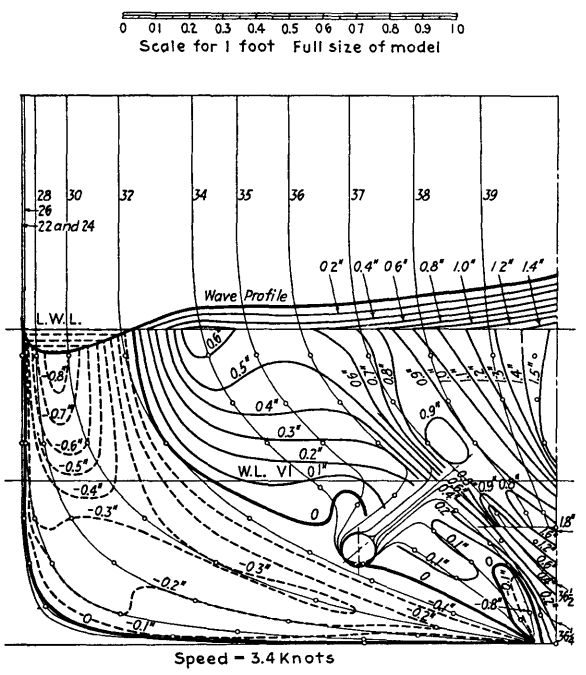

Figure 29

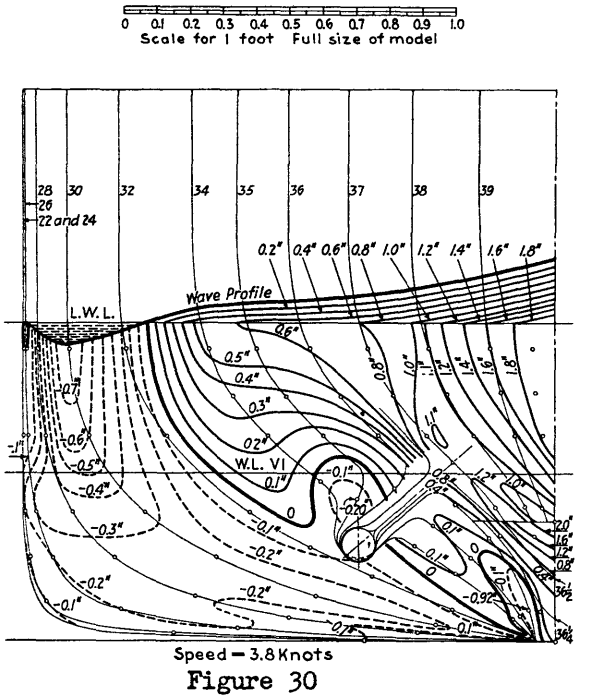

Figure 30

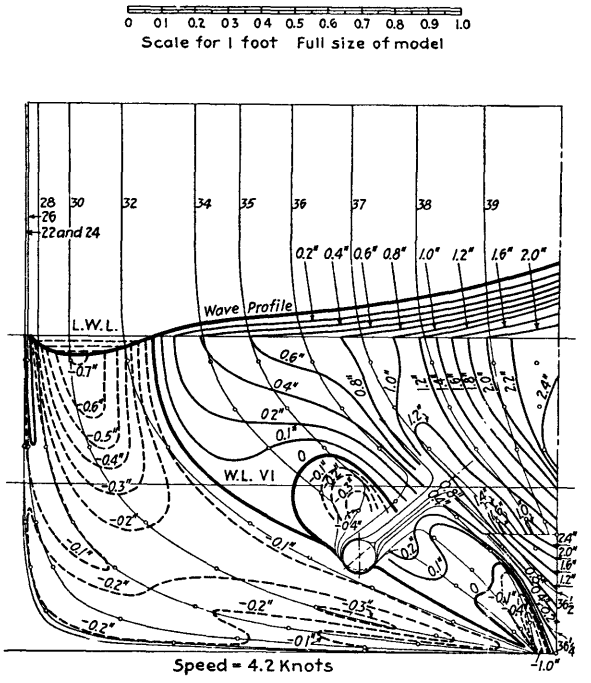

Figure 31

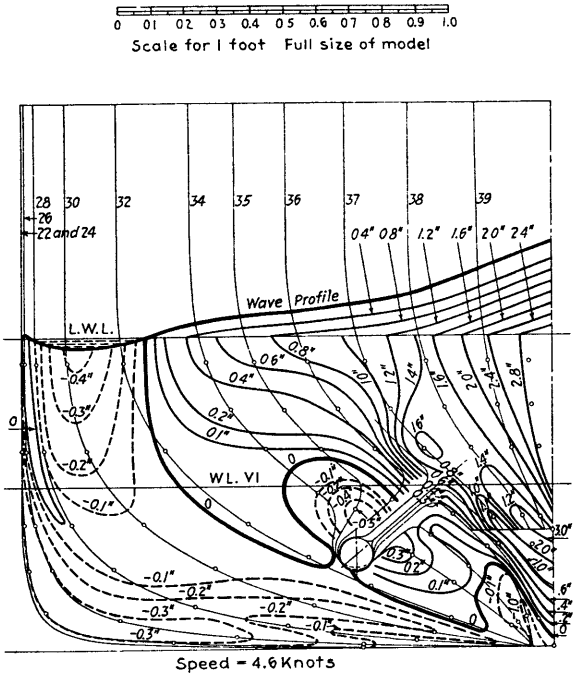

Figure 32

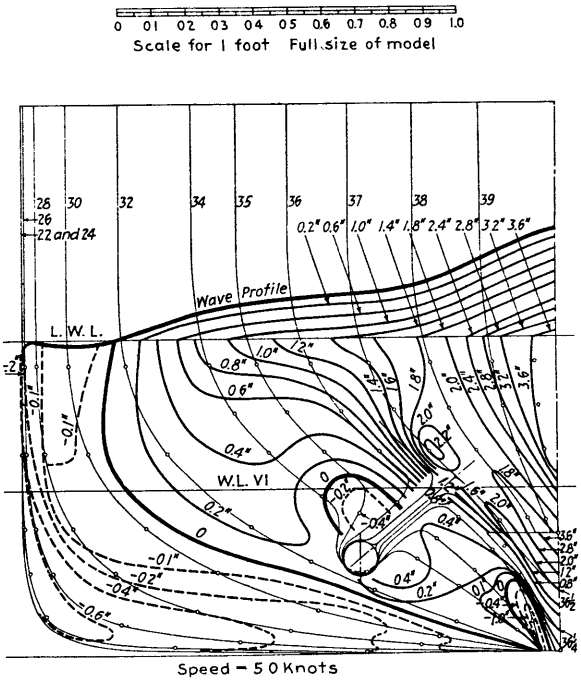

Figure 33

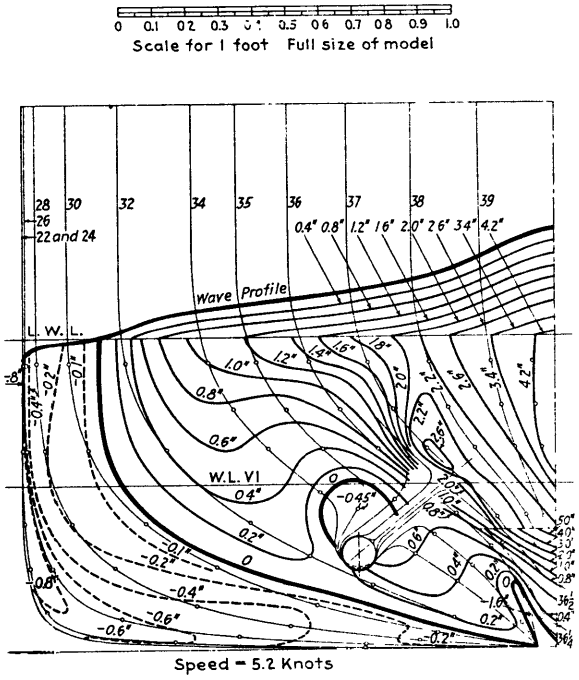

Figure 34

Contours of Change of Pressure on Afterbody

Half body plans of Model 3383, showing contours of change of pressure occurring from the position at rest to various model speeds. Positive pressures indicate an increase in pressure above that existing in the static condition. Small circles indicate the positions of the orifices. All pressures are expressed in inches of water.

pressure changes on the after side of the bulb from Station 3/4 to Station 4. Contours of this type were drawn for seven selected model speeds.

Since the observed pressure values at the orifices represent water pressures normal to the outer surface of the model at those points*, the components of those pressures parallel to the direction of motion of the model may be summed up and resolved directly by measuring the areas between the pressure-contour lines as projected upon the transverse maximum section plane. The full contour lines on the figures represent regions of positive pressures; the broken lines represent negative pressures which tend to reduce the resistance on the bow and increase it on the stern.

DISTRIBUTION OF PRESSURE ON BODY PLANS

By partial summations of pressure changes taken from the contour sheets, it is possible to find the longitudinal forces which act on various parts of the model. In the analysis of the form resistance, all such component resistances have been referred to the total measured (towed) resistance of the model, since this is the criterion of its form which can be most accurately determined and which gives the clearest picture of the quantitative value of the forces involved.

1. The Forward Side of the Bulb – Figures 7 to 13.

The contour of zero change in pressure is practically fixed in position throughout the range of speed. The pressure change on the area inside this contour, and consequently the corresponding force, increased approximately as the square of the speed.

Immediately aft of this area is a band upon which the pressure was reduced. These two areas contain the points at which the greatest pressure changes were measured.

The area of positive change accounted for a retarding force averaging 40 per cent of the total resistance of the model. The average force on the area of reduced pressure, which acted to draw the model ahead, was equivalent to 17 per cent of the resistance. Both these areas contain closed contours surrounding the points of maximum pressure change. Figure 35 shows the summation of the longitudinal forces in this region.

2. After Side of Bulb – Figures 14 to 20.

These figures show the body plan of the model below Waterline VI from Section 3/4 to Section 4. As the sections cross each other, positive changes of pressure in the upper parts of these charts increase resistance while in the lower parts, representing the after side of the bulb itself, positive pressure changes diminish

---

* The absolute truth of this statement remains to be proved, but its validity has been assumed by all experimenters in research of this kind, whether conducted in water or in air.

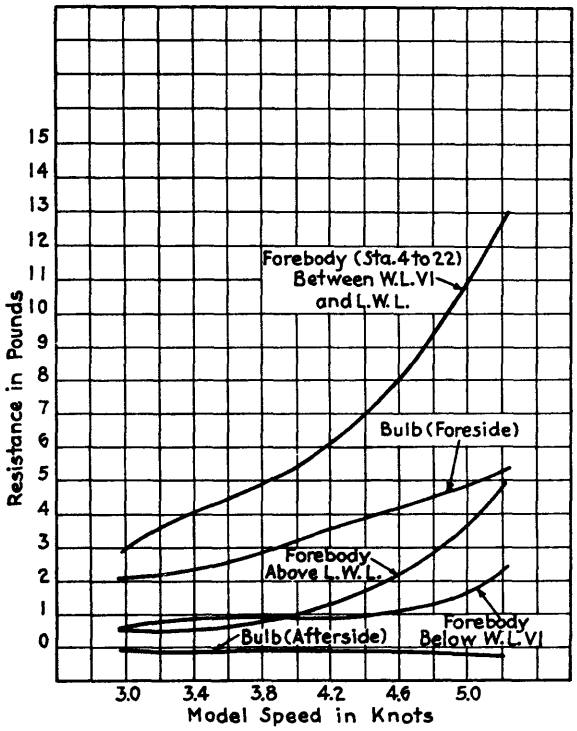

Figure 35 – Form Resistance Contributed by Parts of Forebody

Note the relatively large resistances of the forward part of the bulb and of the forebody above the load waterline, also that the net resistance of the afterside of the bulb is negative.

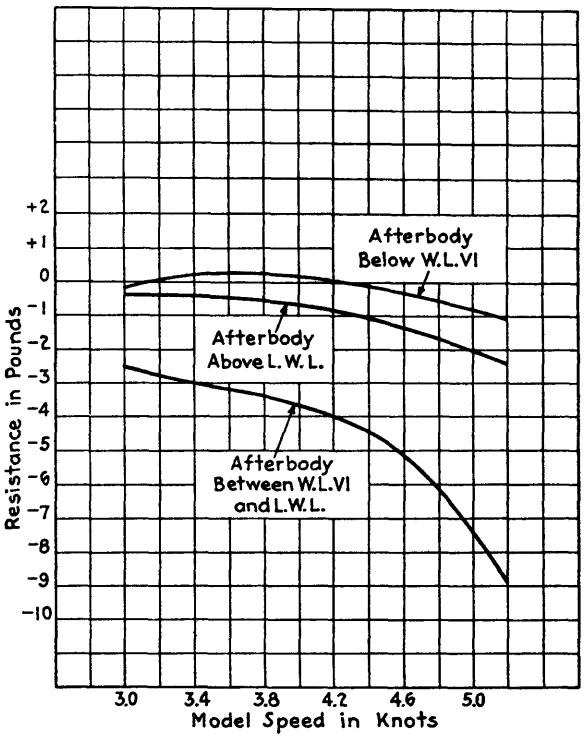

Figure 36 – Form Resistance Contributed by Parts of Afterbody

Note that at low speeds there is a slight positive resistance in the afterbody below the 6-inch waterline.

the resistance. At all speeds the pressure change on the upper part nearly balances that on the lower part. It is to be noted that the line of zero change of pressure is again practically fixed in position throughout the range of speed.

At the lower speeds the areas of maximum change appeared well underneath the model. As the speed increased, the contours defining these areas gradually extended around the turn of the bulb, and at the higher speeds the contours followed the section lines approximately.

3. The Forward Body – Figures 21 to 27.

Discussion of the distribution of pressure changes in the forebody is conveniently separated under three headings:

(a) Below Waterline VI and aft of Station 4;

(b) Between Waterline VI and the load waterline; forward perpendicular to amidships;

(c) Above the load waterline, forward perpendicular to amidships.

In the discussions which follow, the components of total force on the model are given in values which are averaged for the seven model speeds:

(a) In this area the pressure changes were comparatively small and seemed to bear little relation to the speed. The retarding force averaged 12 per cent of the resistance. It was partly balanced by a force on the part of the hull under reduced pressure which averaged about 5 per cent. The net force contributed by this area was therefore quite small.

(b) This portion of the model was subjected to fairly high values of increased pressure over a large area. The retarding force amounted to 48 per cent of the resistance, while the opposite force due to decreased pressure averaged only 5 per cent.

The band of negative change in pressure found on the forward side of the bulb extends up into the area above Waterline VI. Its extent increases with speed until at 4.6 knots it crosses the load waterline and connects with the area of negative change above the load waterline. The fore and aft position of this area of negative change remains practically the same throughout the range of speed.

The number and positions of the points of maximum change of pressure vary with the speed. At 3.0 knots there are two points of maximum positive change and two points of maximum negative change. At 5.0 knots the lesser maxima have disappeared, leaving one positive and one negative, both of which have moved aft.

The pressure wave described under (c) following is also evident below the load waterline, but the secondary undulations seem to become smaller as the distance below the load waterline increases.

In the area of negative change of pressure it may be seen that as the speed increases the contours approach the section lines and the area enclosed by a given contour becomes increasingly narrow at the top. At 5.2 knots the area inside the -1.2-inch contour is wider at Waterline VI than at the wave profile, and a closed contour appears (-1.6 inch) which has a greater value than the depth of the wave profile below the load waterline. This appears as an effort of the water to leave the skin of the model, such as is evident at the extreme bow.

(c) The contours over the area above the load waterline show, for most of the bow wave, a pressure change smaller than that indicated by the wave height. This discrepancy is increased with an increase in speed, especially near the forward perpendicular, until at 5.2 knots

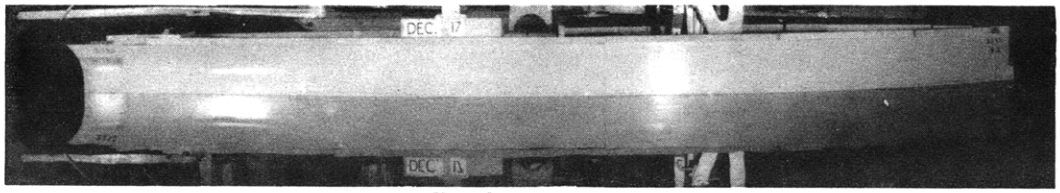

V = 0

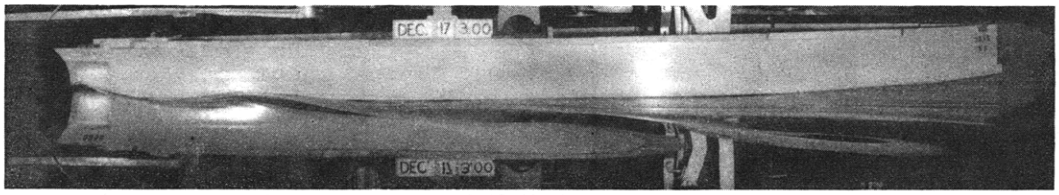

V = 3.00 Knots

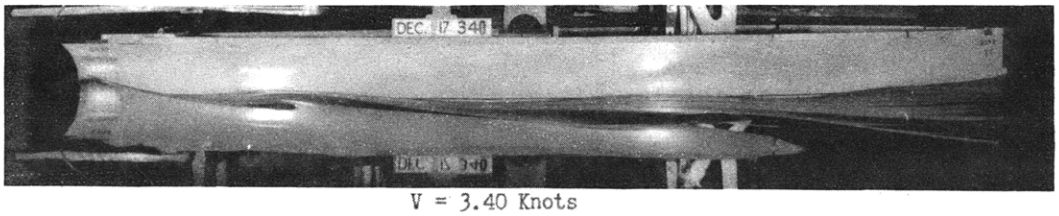

V = 3.40 Knots

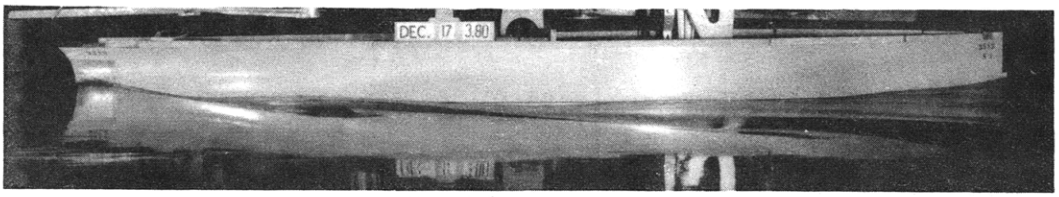

V = 3.80 Knots

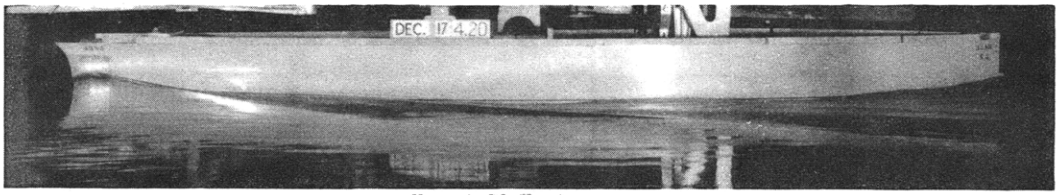

V = 4.20 Knots

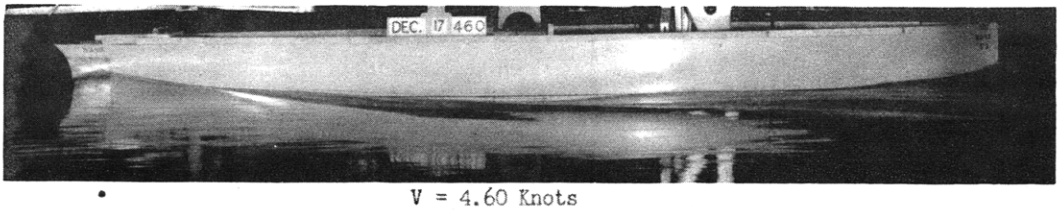

V = 4.60 Knots

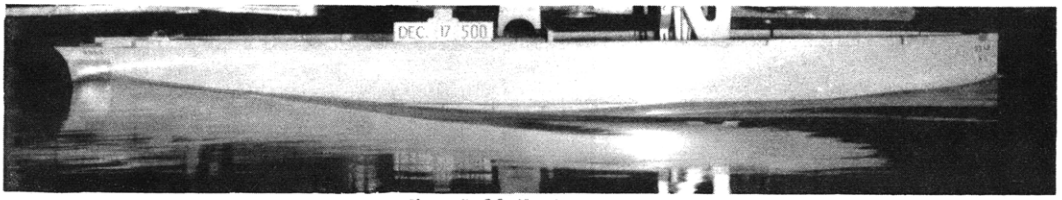

V = 5.00 Knots

Figure 37 – Wave Profiles of Model 3383 at various speeds.

there is very little relation between the height of the wave profile and the pressure change in the 12 inches of length from the forward perpendicular to Station 2.

A careful examination of the bow waves on the photographs, Figure 37, may explain this. The crest of the bow wave is a comparatively thin film of water. The true wave does not rise so far forward nor so high.

It is to be noted also (see Figure 38) that within the bow wave there is a pressure wave of much shorter length. This pressure wave starts with a very high crest at, or forward of, the extreme bow. The first hollow at Stations 1/16 to 1/8 shows a negative change in pressure, which, for this area above the load waterline, means a pressure less than atmospheric.

The number of wave crests following the first or bow wave crest varies from one at 3 knots to three at 5 knots. It was observed that, however smooth the water in the basin might be, the bow wave was in constant vertical motion as though the model were meeting a series of waves.

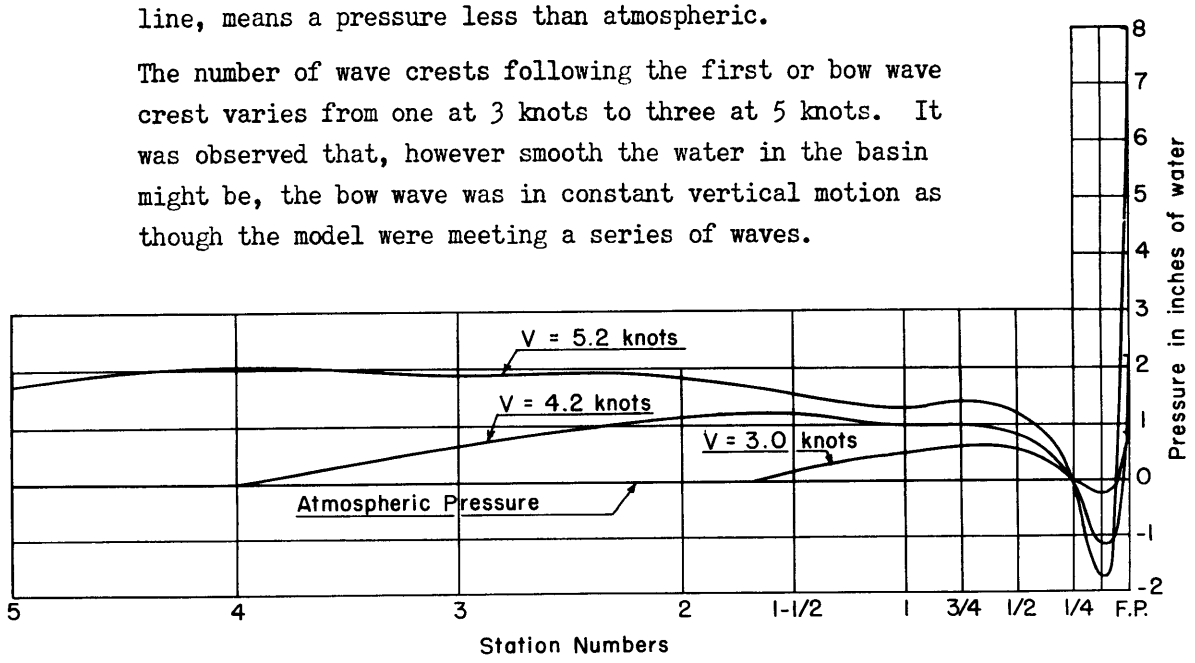

Figure 38 – Curves Showing Change of Pressure along a Waterline 0.17 inch above the Load Waterline. The Diagram Illustrates the Pressure Wave within the Bow Wave.

The area covered by the bow wave was the only one on which the proportion of the net force to the total resistance varied with speed to any great extent. This rose from 7 per cent at 3.0 knots to 17 per cent at 5.2 knots; that is, it increased with the bow wave.

4. The Afterbody – Figures 28 to 34.

The afterbody was analyzed in three parts in the same manner as the forebody. The analysis of the afterbody is shown in Figure 36. It is to be noted in these figures that positive changes in pressure decrease the resistance of the model.

(a) Below Waterline VI.

The small changes in pressure over this part of the hull and over the areas of increased and decreased pressure nearly balanced, contributing very little to the resistance.

(b) Between Waterline VI and Load Waterline.

The largest part of the force acting to reduce resistance was found to be applied to the part of this area which showed increased pressure. It averaged about 33 per cent of the total resistance of the model.

The concentration and peculiar shape of the contours around the after part of the bossing are discussed later under "Contours on Shell Expansion."

(c) Afterbody Above Load Waterline.

The positions of the contours over this area were estimated, as there were no orifices above the load waterline in the afterbody. Moderately high changes of pressure were recorded near the stern, but the areas involved were small. The forward force, which reduced resistance, was equivalent to about 5 per cent of the total resistance.

SUMMARY OF LONGITUDINAL FORCES

The principal part of the retarding force was applied upon two areas:

1. The forward end of the bulb on the bow, which contributed a force averaging 40 per cent of the total resistance;

2. The forebody between Waterline VI and the load waterline, upon which the force averaged 48 per cent of the total resistance.

The advancing or assisting force was also applied on two areas:

1. The band of reduced pressure on the forward side of the bulb, which produced a force equivalent to 17 per cent of the total resistance;

2. The area of increased pressure in the afterbody between Waterline VI and the load waterline, which produced a force equivalent to 33 per cent of the total resistance.

The algebraic sum of these four forces, averaged for the seven model speeds, is 38 per cent of the measured total resistance of the model. As a general comparison of magnitudes, the proportion that the calculated residuary resistance bears to the measured total resistance increases with the speed, from 32 per cent at 3.0 knots to 52 per cent at 5.2 knots.

Lines of flow of water are from tests of bare hull at 4.8 knots. (A) ——— - ——— - ———

Lines of flow with appendages at 4.2 knots. (B) - - - - - - - - - -

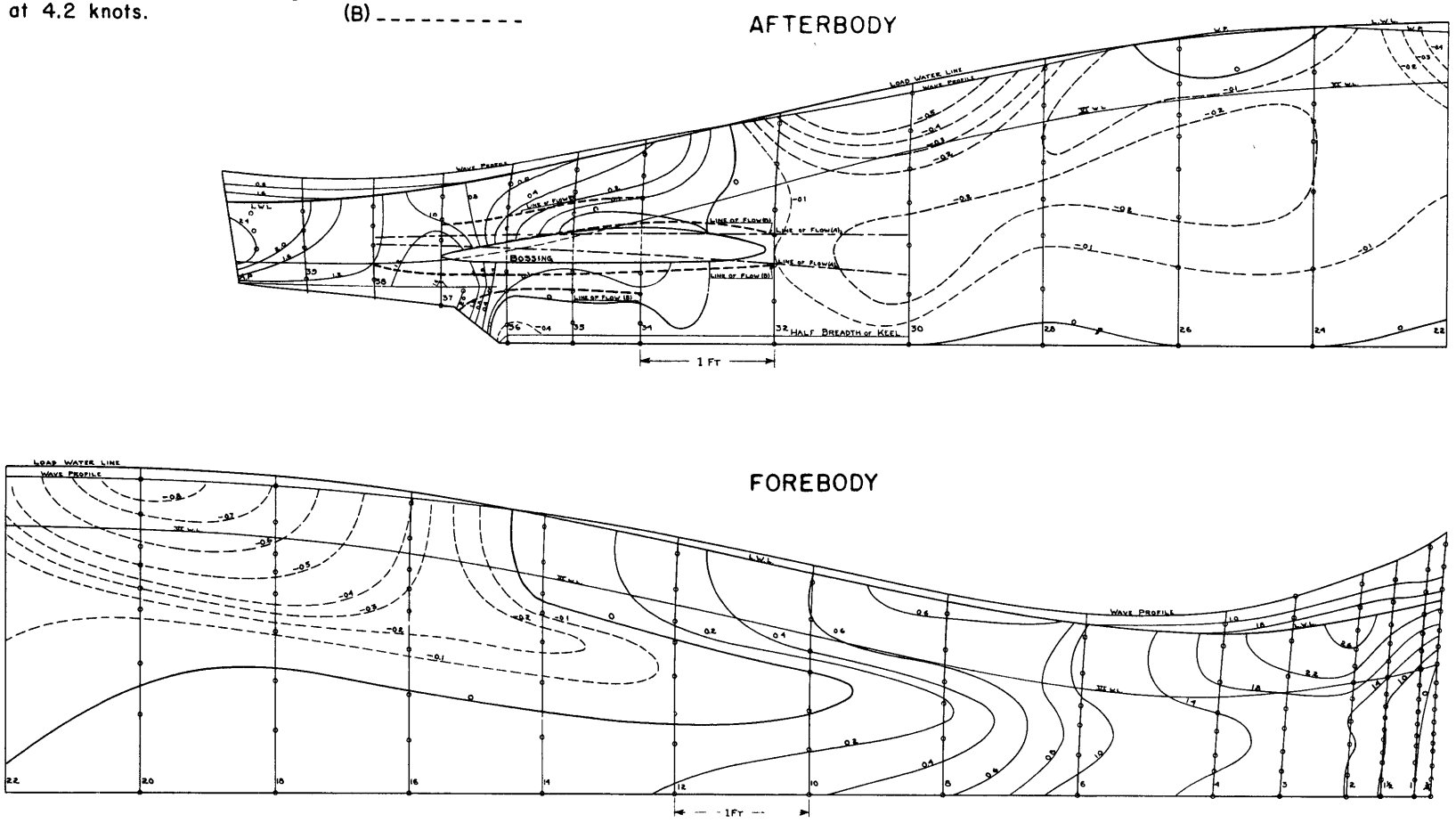

Figure 39 – Wetted Surface Expansion of Model 3383, showing Contours of Change of Pressure in Inches of Water due to Speed of 4.2 Knots.

CONTOURS ON SHELL EXPANSION

Figure 39 is an expansion of the wetted surface of the model, with contours of change of pressure drawn upon it. Several lines of flow are also shown in the vicinity of the bossing.

The pressure contours and the lines of flow around the bossing correspond to a speed of 4.2 knots. The two lines of flow over the bare hull were determined for a speed of 4.8 knots, but the relation between them and the contours of pressure in way of the bossing probably holds throughout the range of speed tested, since the general pattern of the contours is constant in that vicinity.

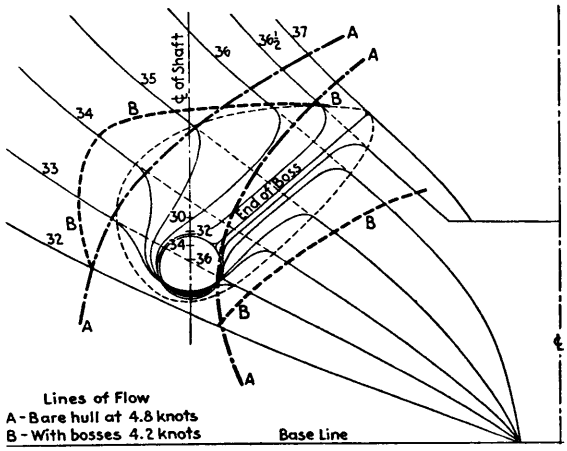

Figure 40 – Model 3383: Bossing–Stern No.3 – S_2

This pattern shows the effect of placing the bossing in the line of flow or across it. The forward part of the bossing is in the line of flow and the contours of pressure in that region are wide apart and nearly symmetrical. The after part of the bossing was purposely not curved to follow the streamlines and the effect is obvious in the change in direction and crowding together of the contours. Figure 40 shows the streamlines on the body plan in the vicinity of the bossings.

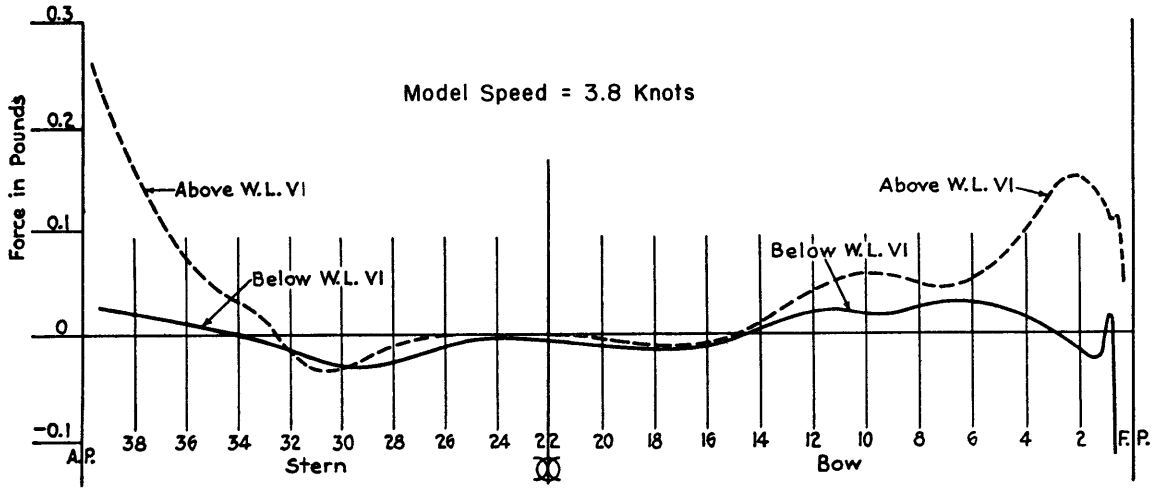

Figure 41 – Curves of Longitudinal Force Per Inch Length

Waterline VI is 6 inches above the base line of the model. Positive forces on the bow increase the resistance of the model; positive forces on the stern decrease it.

LONGITUDINAL DISTRIBUTION OF THE FORCES – Figures 41 and 42.

The scale for forces in Figure 41 is 20 times that in Figure 42, which indicates the extreme values of the forces acting on the forward side of the bulb.

Exclusive of the bulb, the principal forces are shown to be acting on the portion of the model above Waterline VI in both the forward and after bodies.

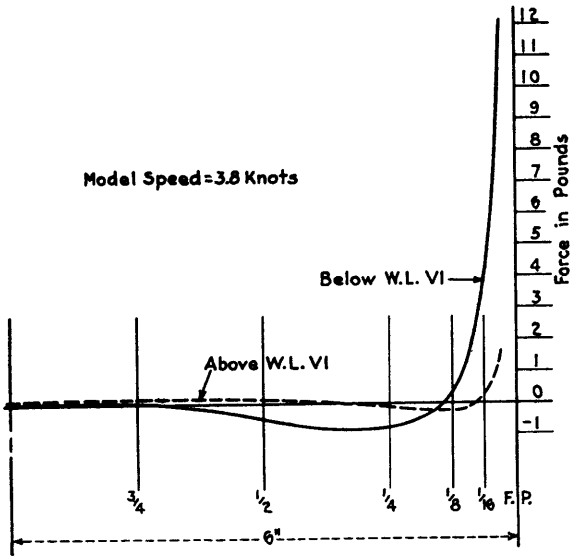

Figure 42 – Longitudinal Force Per Inch Length at Extreme Bow

Positive forces increase the resistance of the model.

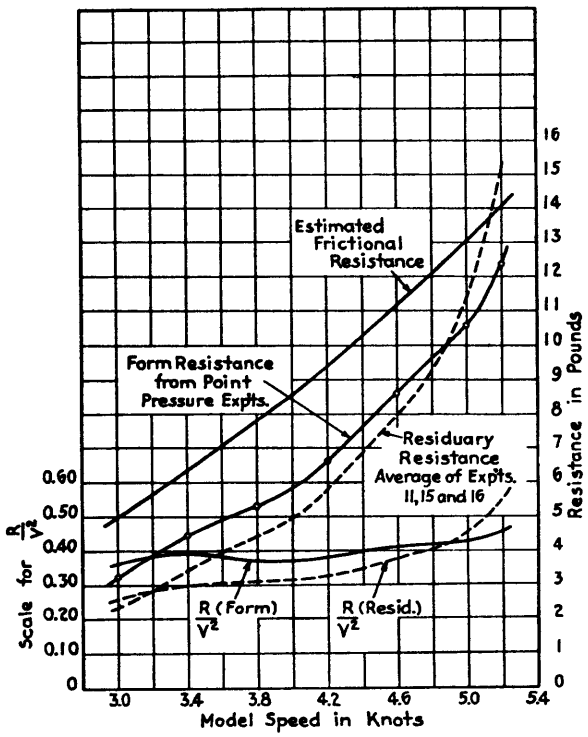

Figure 43 – Curves of Form Resistance, Residuary Resistance and Specific Resistance

The values for the form resistance curves are taken from the point pressure experiments. Those for the residuary resistance curves are computed from towing experiments Nos. 11, 15 and 16 on Model 3383.

FORM RESISTANCE

The form resistance of the model was computed by summation of the longitudinal forces over the body plan of the model for seven different speeds. These values and the curve through the spots are shown in Figure 43. This curve is compared with the curve of residuary resistance obtained in the usual way, using Gebers' coefficients when estimating the frictional resistance, and using for total resistance the average of three towing tests.

The relation between these two curves is opposite to that found by Laute for a merchant ship form*, but that it is not accidental is indicated by a

---

* "Untersuchungen uber Druck und Strömungsverlauf an einem Schiffsmodell" (Investigations of Pressure and Flow on a Ship Model), Dr. Eng. Wilmar Laute, Schiffbautechnische Gesellschaft, Volume 34, 1933. (Experimental Model Basin Translation 53).
This reference gives in detail the results of point pressure and velocity measurements, together with an analysis of the form resistance obtained from the experiments and also comparisons with calculated residuary resistances.

comparison with the results of a previous point pressure test†.

Form resistance obtained by point pressure is compared with calculated residuary resistance in Figure 44, for both Models 2861 and 3383. All the resistances are expressed in fractions of the total resistance of the model. Although the speed range of the tests of Model 2861 was restricted to the higher speeds, the directions of the curves agree with those of Model 3383 to indicate that the proportion of form resistance from point pressure is higher at low speeds and lower at high speeds than that of the calculated residuary resistance. That the curves for Model 2861 cross at a lower speed than the similar crossing for Model 3383 is explained by the fact that the resistance curve of Model 2861 started up on its steep slope (indicating sharply increased residuary resistance)

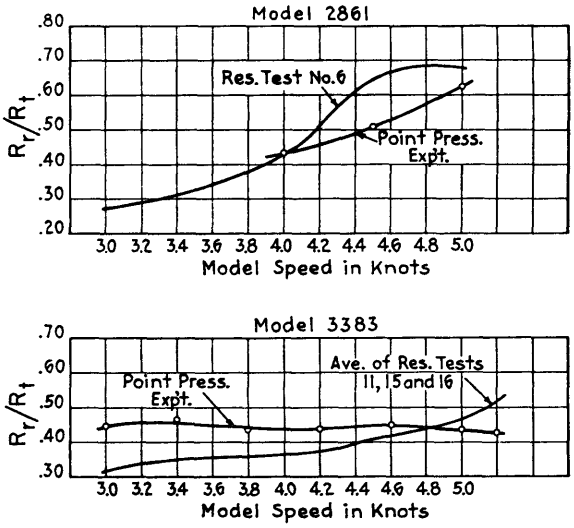

Figure 44 – Comparison of Form and Residuary Resistance for Models 2861 and 3383

The form resistances are taken from results of the point pressure experiments. The residuary resistances are derived from the results of towing tests in the usual manner, by subtracting the estimated frictional resistance from the total observed resistance. Both sets of values are expressed in fractions of the total observed resistance.

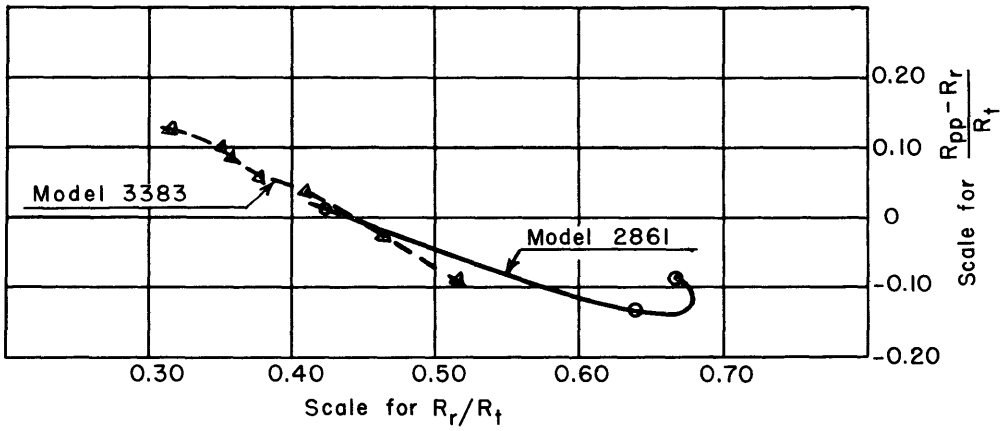

R_t = Total Resistance (measured)

R_{pp} = Form Resistance Found By Point Pressure

R_r = Residuary Resistance Computed By Use Of Gebers' Formula For Frictional Resistance

Figure 45 – Difference Between Residuary and Form Resistances in Proportion of Total Resistance

† "Form Resistance Experiments", by Captain E. F. Eggert, (CC), U.S.N., Transactions, Society of Naval Architects and Marine Engineers, Vol. 43, 1935, pp. 139-150.

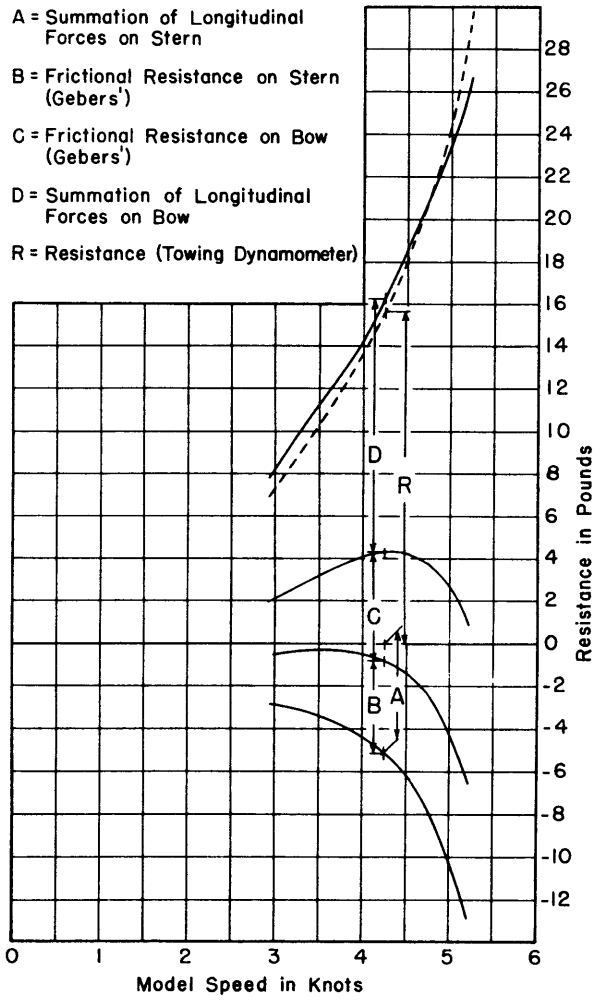

Figure 46 – Comparison of Estimated and Measured Resistances

at a speed of 4.0 knots, while the change in slope of the resistance curve of Model 3383 was more gradual, occurring at nearly 5.0 knots. To illustrate this agreement more clearly, the differences between form and residuary resistances were plotted in proportion to total resistance in Figure 45.

A final chart of comparison of the estimated and measured resistances is shown in Figure 46. From the base line, the form resistance of the stern is laid off as ordinate (A). From this curve as a base, the estimated frictional resistance of the stern is added (B).

This plot illustrates the fact that at all speeds between 3.0 knots and 5.2 knots the stern is not only overcoming its own frictional resistance but also some of the frictional resistance of the bow.

Continuing in this manner, the frictional resistance of the bow (C) is added, and to this is finally added the form resistance of the bow (D). The result is the total resistance of the model as given by the sum of the net form resistance and the frictional resistance computed by Gebers' formula. This is compared with the actual measured resistance, which it exceeds at the lower speeds; at speeds above 4.75 knots, however, the measured resistance is greater.

SELF-PROPELLED TESTS

A second set of tests was carried out to measure the effect of the propellers on the hull. The model was tested self-propelled in the usual manner, using propellers 1415 and 1416, of diameter 6.76 inches and pitch 6.72 inches; see Table 2 (page 3) and Figure 47.

Twenty-five additional orifices were arranged around the bossing, skeg, fairwater, and extreme stern. These, with 32 of the orifices previously tested, covered the area from Station 30 to the stern, or 5 feet of the length of the model,

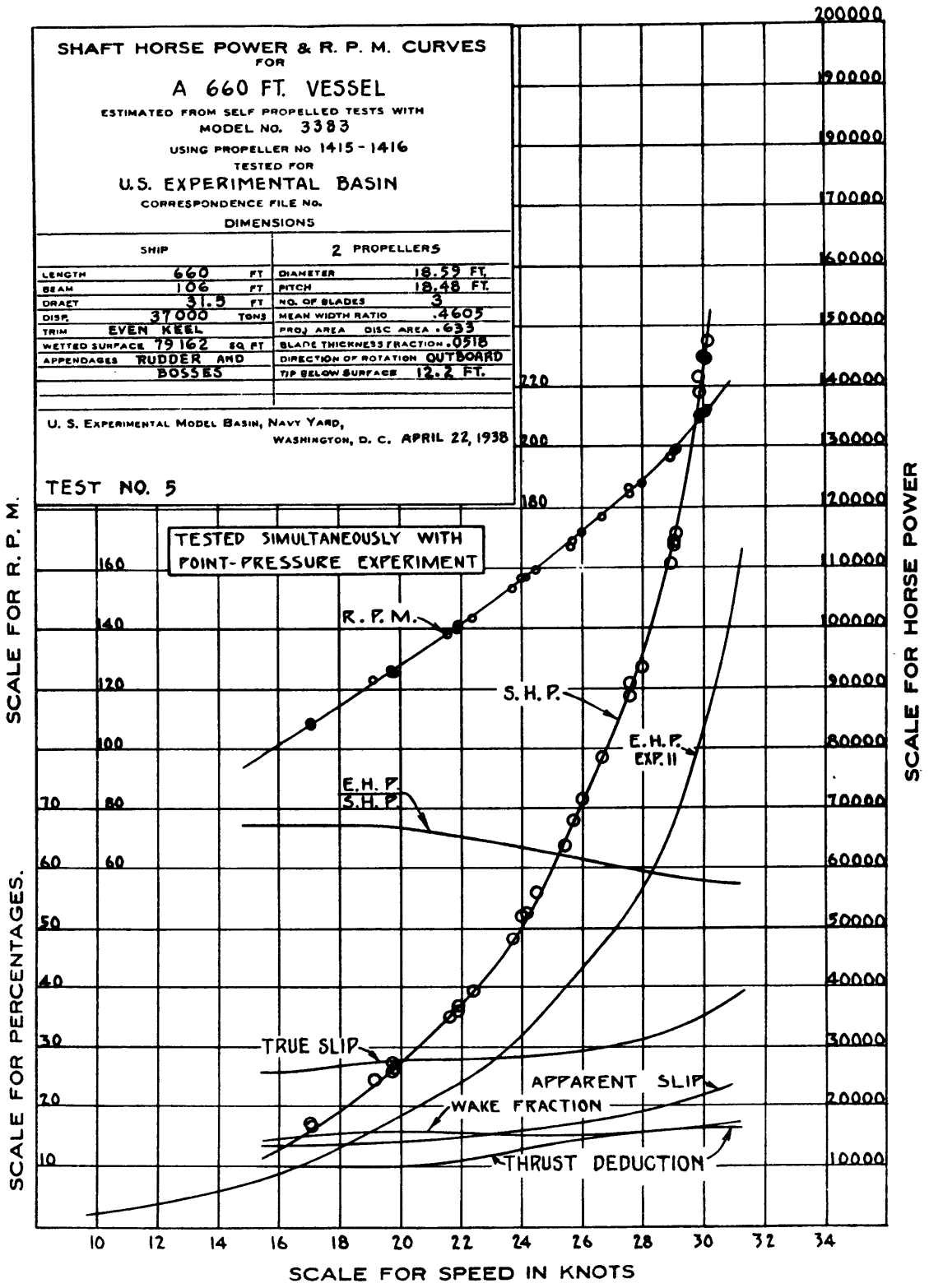

Figure 47 – Self-propelled Tests with Model 3383, showing Curves of SHP and RPM for a 660-foot Vessel

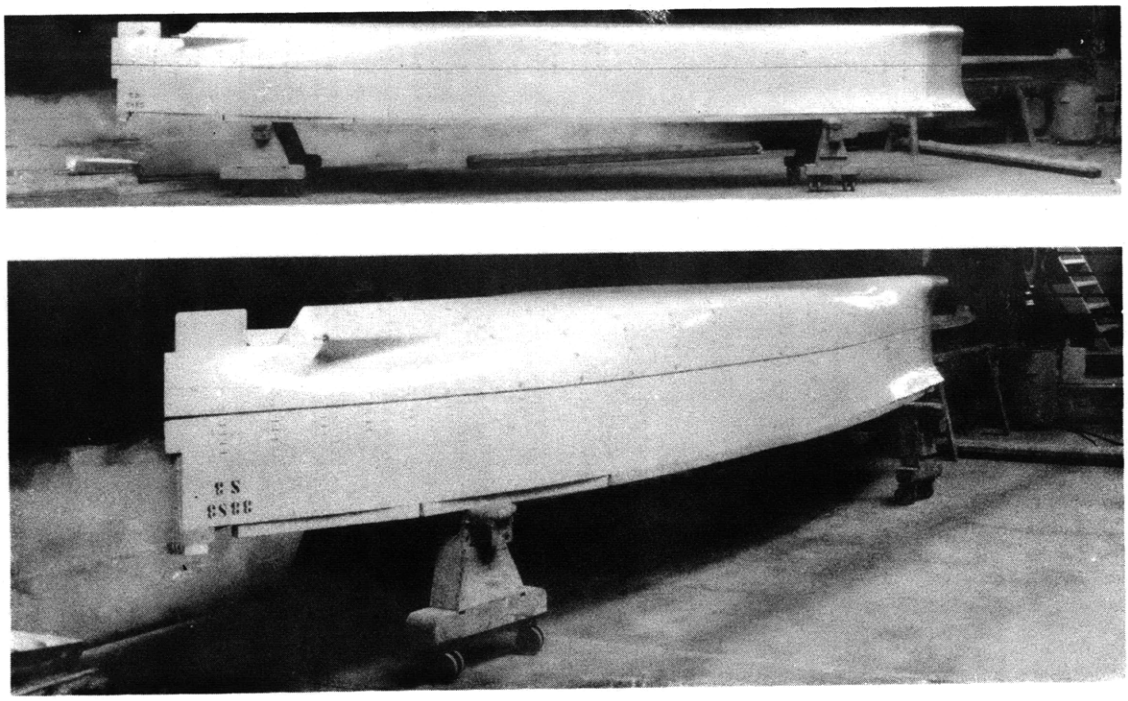

Figure 48 – General Views of Model 3383

The orifices for pressure measurements are located in the centers of the large disks on the surface of the model.

as shown in Figure 48.

Pressure changes at these orifices were measured while the model was self-propelled and also while it was towed with the propellers removed. The curves of pressure change were faired as before and the difference between the pressures under the two conditions were plotted as contours of pressure on the body plan. Consequently, these contours, Figures 49 to 55, show the thrust deduction as measured by point pressure for each of the seven speeds.

It should be noted that the pressure changes shown on these sheets are relative to the condition "propeller off," and not to the condition of rest. Thus the line of zero change in Figure 49 indicates that the pressure recorded was the same as that shown in the corresponding position in Figure 28, and that the working of the propellers produced zero change along this contour.

The pressure changes produced by the propellers are small and they affect a comparatively small area, insofar as pressure changes within the limits of accuracy of the apparatus are concerned.

These pressure changes were summed up for each speed. Figure 56 shows a comparison of the values of thrust deduction found by point pressure with those obtained in the usual manner by self-propulsion tests. The point-pressure method shows less than half the calculated thrust deduction. It is possible that this is due, in

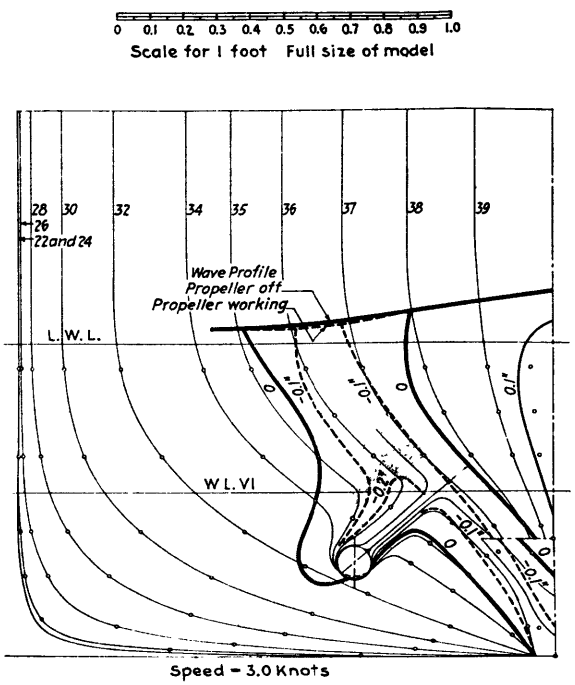

Figure 49

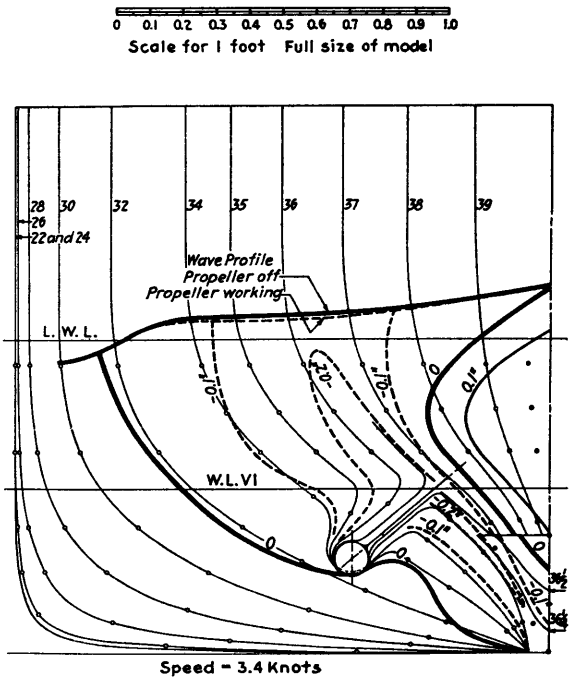

Figure 50

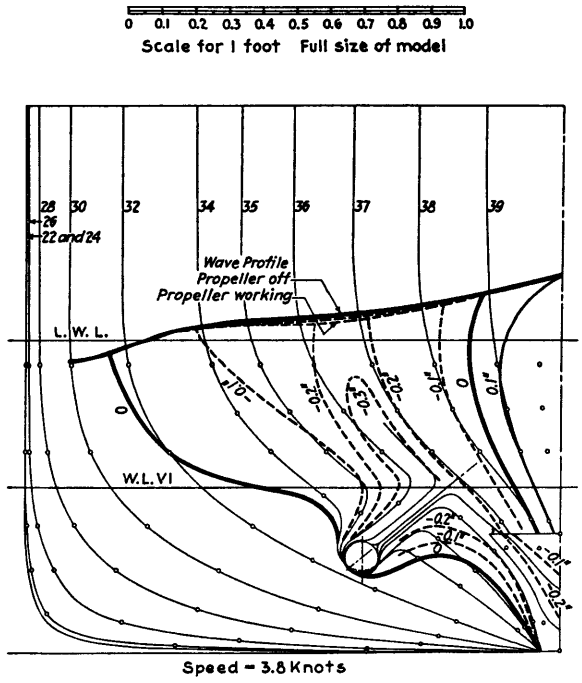

Figure 51

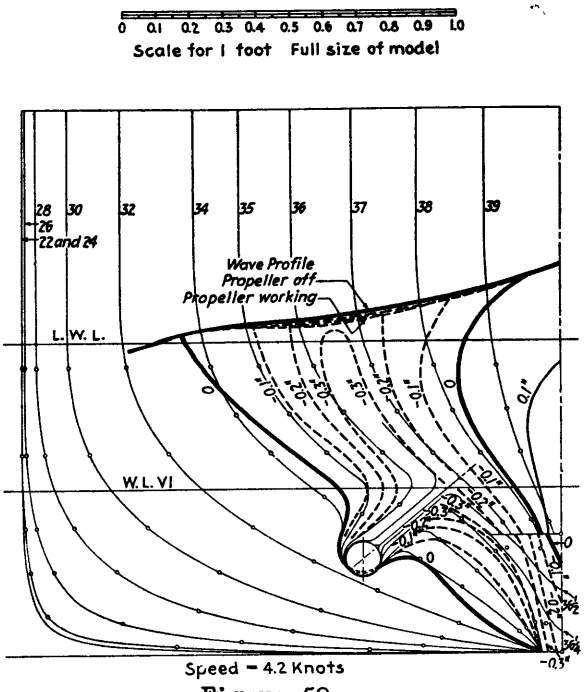

Figure 52

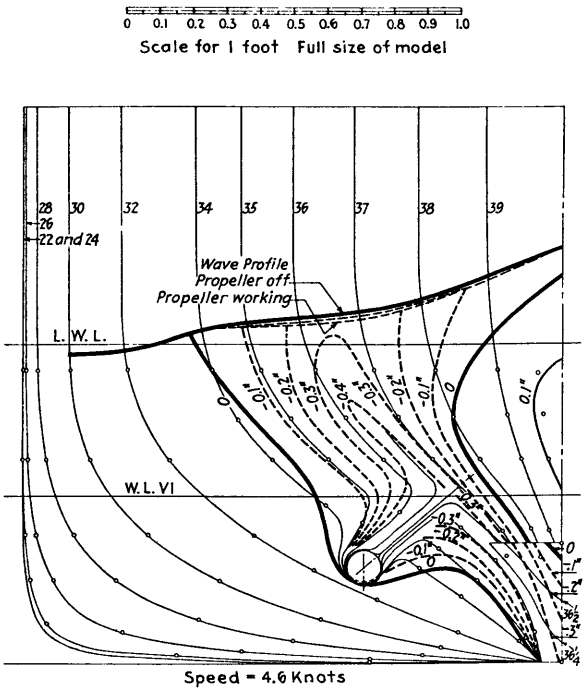

Figure 53

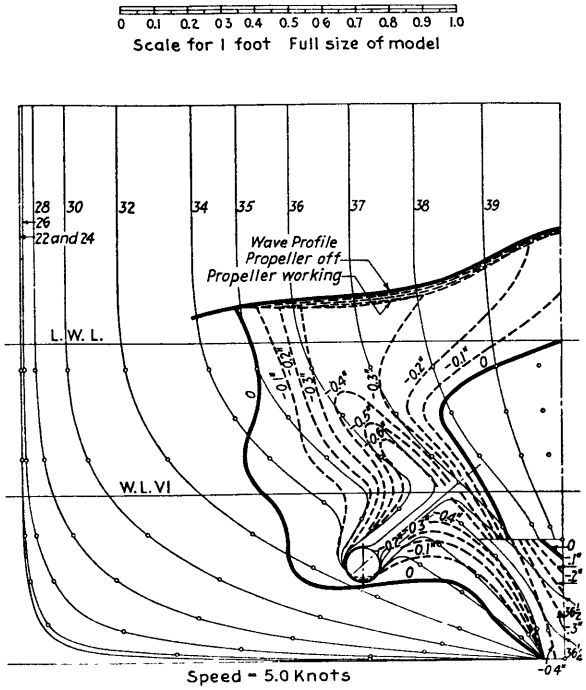

Figure 54

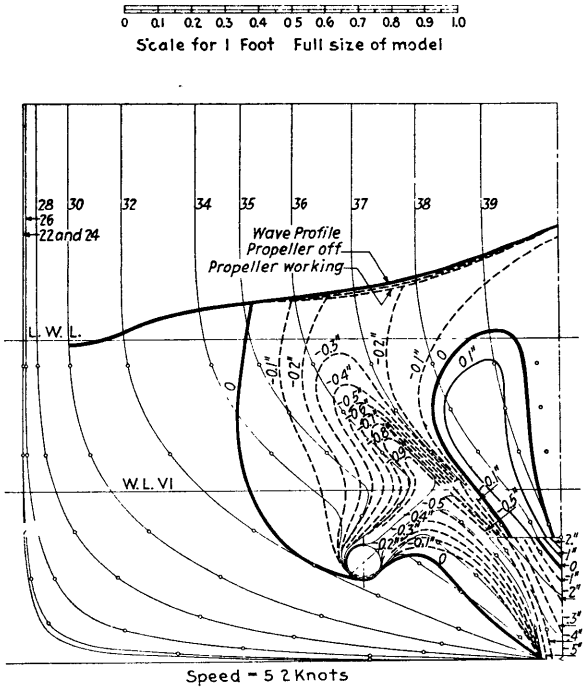

Figure 55

Contours of Change of Pressure on Afterbody Representing Differences Between Towed and Self-Propelled Conditions

Half body plans of Model 3383, showing contours of changes of pressure occurring from the towed to the self-propelled model conditions. Positive pressures indicate an increase in pressure above that existing in the towed condition. Small circles indicate the positions of the orifices. All pressures are expressed in inches of water.

part, to changes of pressure (probably too small to measure with the apparatus) spread over large areas. It is also to be noted that the areas of greatest change of pressure, on the ends of the bossings, had no pressure orifices. These areas, however, were small.

Figure 57 shows the pressure contours on the expanded surface for the self-propelled condition. Figure 58 is a similar map of the thrust deduction contours.

The contour sheets, Figures 49 to 55, indicate a reduction of pressure under the stern around the propellers. This would cause a change of trim, so the model was tested for change of level, with and without the propellers working. Figure 59 shows the results of these tests, in which a measurable effect of the propellers upon the trim may be observed.

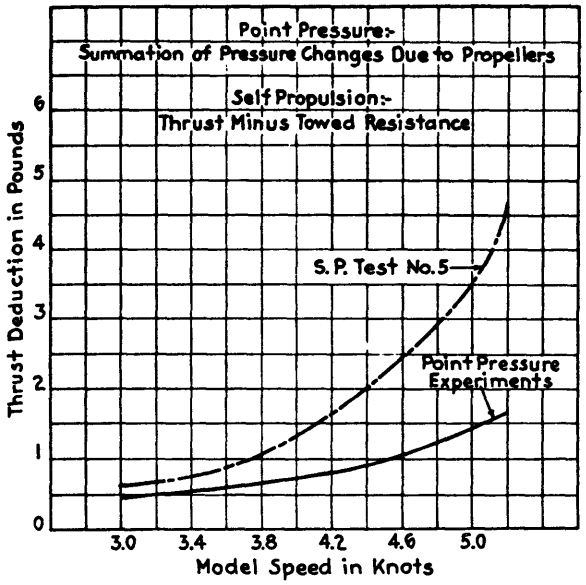

Figure 56 – Curves of Thrust Deduction for Model 3383

The lower curve is derived from point pressure experiments with the model self-propelled. The upper curve is derived from a self-propulsion test in the usual manner by subtracting the observed resistance of the model when towed from the thrust when self-propelled.

SUMMATION OF VERTICAL FORCES

A summation of the vertical forces was also made. For this purpose the contours of pressure were projected on a horizontal plane and the areas between the contours were multiplied by their respective average pressures.

Partial summation of these forces in Table 3 gives the results for a speed of 4.2 knots.

TABLE 3

Areas	Upward Force (pounds)	Downward Force (pounds)
Bulb (upward)	7.36	
Bulb (downward)		9.02
Forebody (positive areas)	20.54	
Forebody (negative areas)		6.24
Afterbody (positive areas)	7.10	
Afterbody (negative areas)		11.39
Totals	35.00	26.65
Net upward force	8.34	

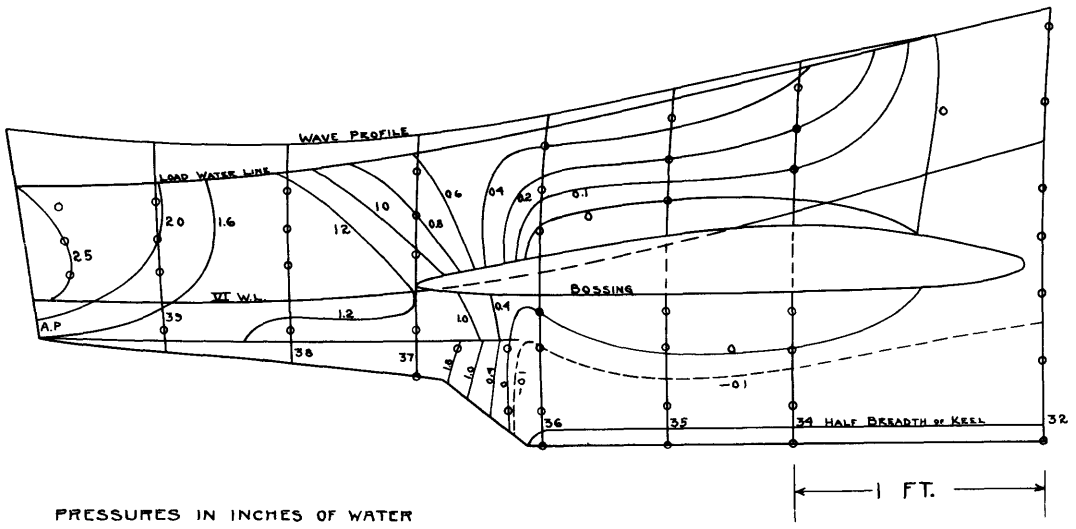

Figure 57 – Wetted Surface Expansion of Model No. 3383, Showing Contours of Change of Pressure due to Speed of 4.2 Knots. Propellers Working.

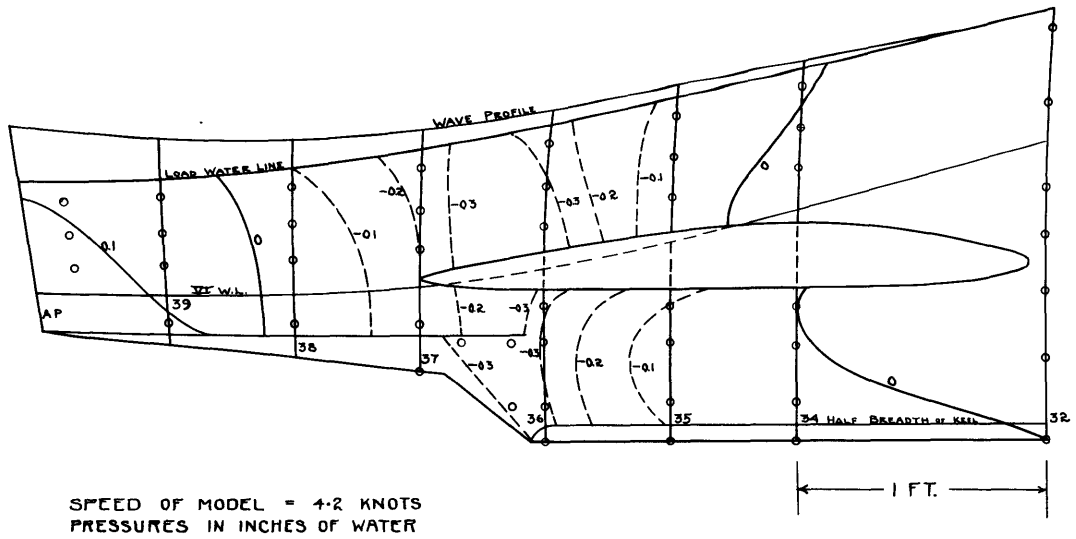

Figure 58 – Wetted Surface Expansion of Model No. 3383, Showing Contours of Pressure Differences due to Propeller Action.

The net dynamic upward force would be balanced, of course, by a reduction of like amount in the displacement, from 2257 pounds to 2249 pounds, or less than 0.4 per cent.

EFFECT OF CHANGE IN FORM OF BULB

After the completion of the experiments previously described, it was decided to determine the effect on the total resistance of a change in the angle of entrance of the waterlines at the bow. Figure 60 shows the lines of the bow as designed and as altered.

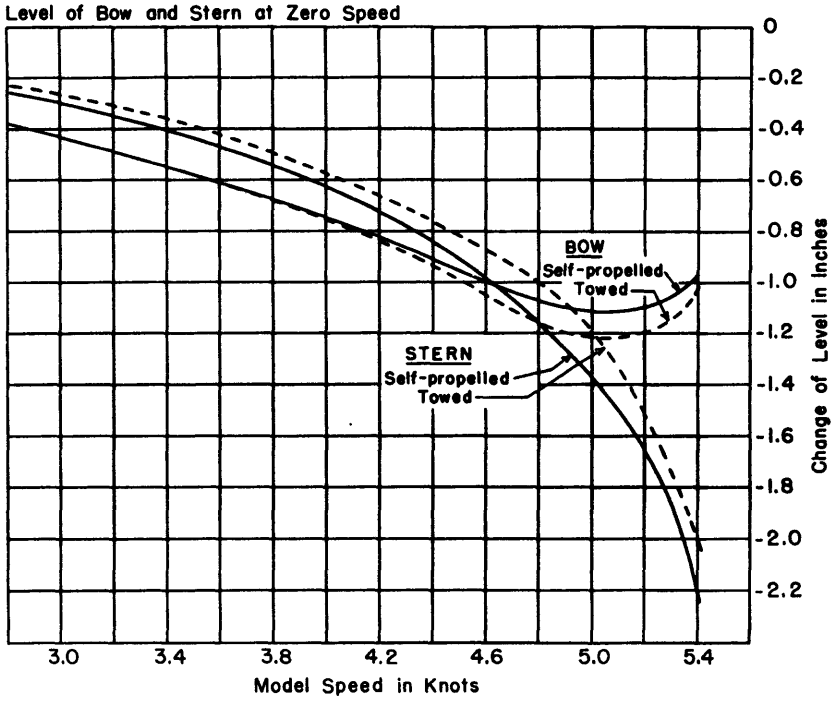

Figure 59 – Curves of Change of Level for Model 3383.

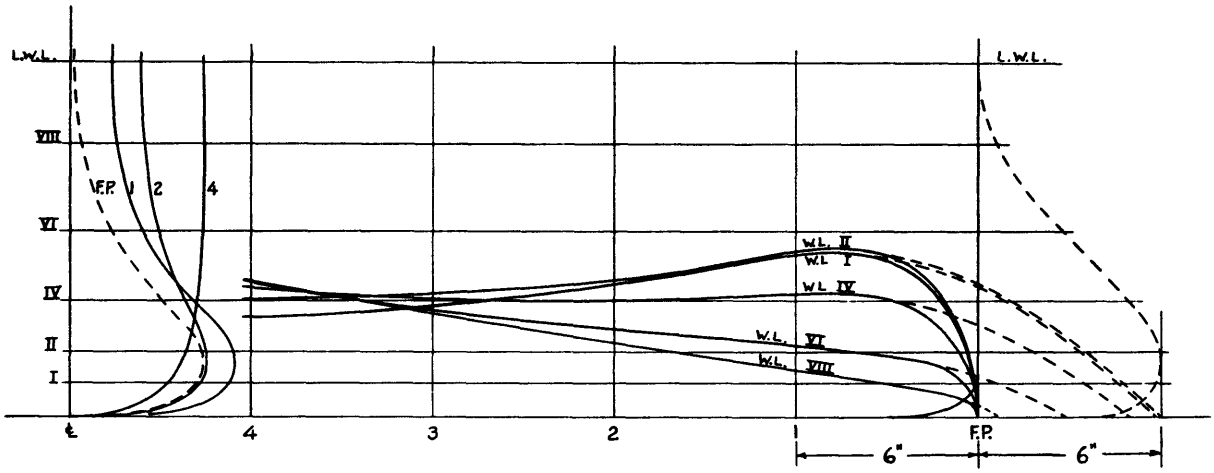

Figure 60 – Model 3383. Lines of Bow.

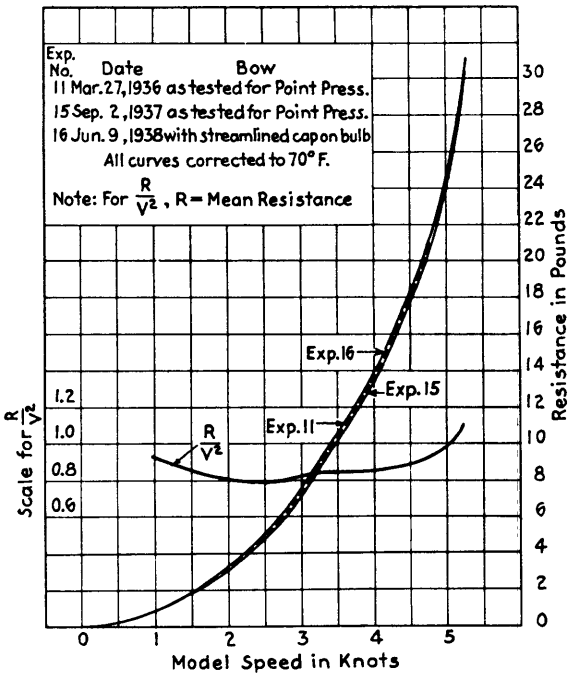

Figure 61 – Curves of Resistance for Model 3383

The resistance curve of the altered bow is shown in Figure 61, where it is compared with two curves obtained with the bow as designed. It is evident that the altered bow did not change the total resistance perceptibly, although it must have altered the pressures around the bow very considerably.

This experiment illustrates the difficulty of obtaining a net gain in total resistance by some local change of form, even though the change is certain to lower the pressure over a selected high-pressure area.

CONCLUSIONS

The contour sheets give a detailed picture of the action of the bulb bow, the bow wave, the bossings, and the thrust deduction around the propellers.

The summations indicate that the form resistance obtained by point-pressure test was greater at low speeds and less at high speeds than the residuary resistance as computed from towing tests in the usual manner.

The point-pressure test with the propellers working indicated that the change in longitudinal force produced by action of the propellers was less than the thrust deduction (or augmentation to the resistance), obtained in the usual way.

ACKNOWLEDGMENTS

The initiative, encouragement and assistance of Captain E. F. Eggert, (CC), U.S.N., (Retired), have served as the inspiration for the work described in this paper.

The painstaking efforts of Mr. S. C. Gover, Assistant Mechanical Engineer, aided greatly in the successful culmination of the experiments.

APPENDIX 1

DESCRIPTION OF TEST APPARATUS

The detail arrangement of orifices, discs, and tubes is shown in Figure 1.

Every effort was made (1) to finish off the discs and tubes to the fair surface of the model; (2) to place the axis of the disc or tube at 90 degrees to the plane tangent to the surface at the orifice, and (3) to avoid any projections or depressions around the edges of the orifices.

The copper tubes were led as directly as possible from the orifice to the deck of the model, where they were connected by rubber tubes to a 30-tube manometer, as shown in Figures 2 and 3.

The glass manometer tubes had an inside diameter of about 1/4 inch, and the glass screen behind the manometer tubes showed horizontal reference lines at intervals of 1 inch, for convenience in taking data from the photographs.

It is estimated that the pressures recorded and observed by this method were accurate to within 0.05 inch of water, except where the duration of a run was insufficient.

In view of the great number of orifices near the bow, and the difficulty of fitting orifices with brass discs, the port side of the bow, for 11 inches back from the forward perpendicular, was formed of a hollow white metal casting, as shown in Figure 1.

In the narrow part of the casting, near the normal waterline, where the orifices were too close together to permit the use of nipples, an improvised manifold connected to a single copper tube was used for each set of four holes. The three holes connecting to this manifold which were not in use at any one time were plugged with plasticine.

The upper end of the manometer was connected to a vacuum tank on the carriage, by means of which the water in the tubes was raised to a height convenient for observation and photography. As the vacuum tank was very large compared to the volume of air displaced in the manometer tube when the water rose or fell from its zero position, the errors due to the use of an elevated water level, and to possible slight leaks in the system, were considered negligible.

The holes above the load waterline were connected to the same manometer but were operated individually by means of the apparatus shown in Figure 62.

Since the manometer was fixed on the model during the readings, no correction was necessary for changes of level of the model.

OPERATION OF THE ORIFICES ABOVE THE LOAD WATERLINE

The operation of the holes above the load waterline was based on the fact observed during a previous test that if a hole was exposed to the air when the height of the water column above it balanced the partial vacuum in the tank, surface tension

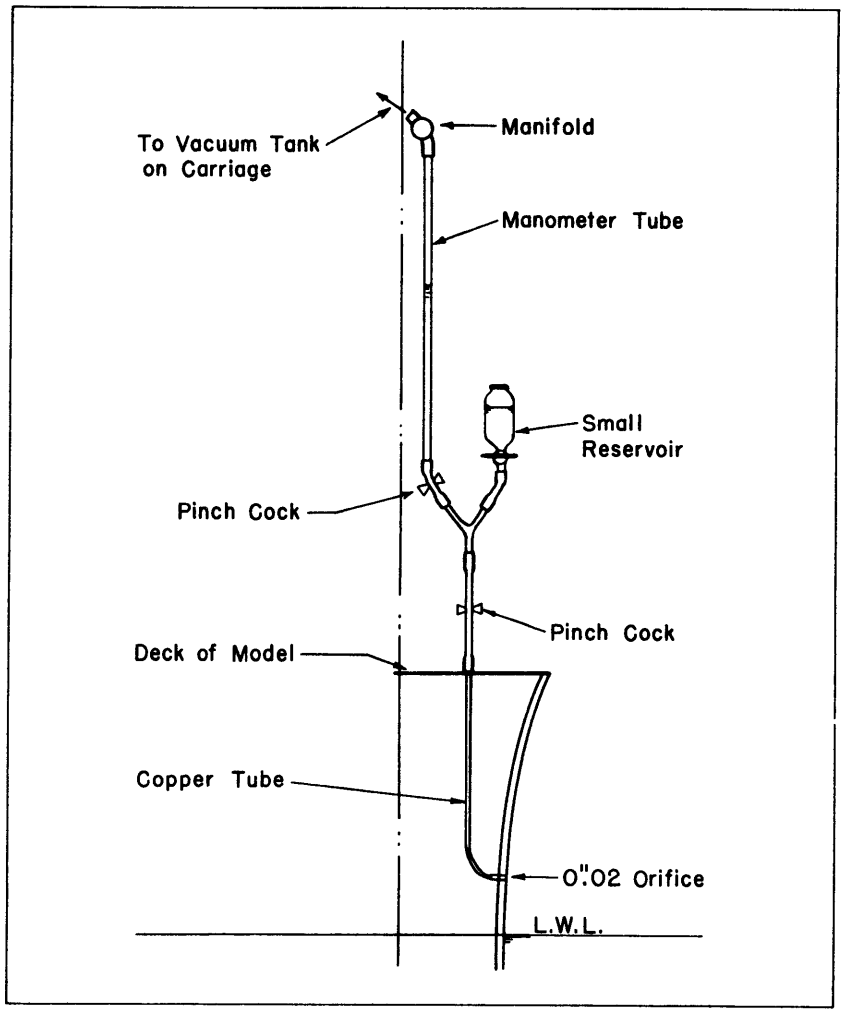

Figure 62 – Apparatus used for Orifices above Load Waterline

would seal the hole and no air would enter or water run out.

In practice, after the air had been worked out of the tubes (Figure 62), the column of water was run up several inches above the level of equilibrium by opening the cocks between a reservoir and the manometer. With the reservoir shut off and the cocks opened between the orifice and the manometer column, the top of the column would slowly sink to the proper height and stop. The orifice was then ready to transmit any change of pressure, since a change could occur only after the orifice had been covered with water, when it would function in the same way as the orifices below the load waterline.

At the end of the run, after a recording photograph was taken, the cocks were closed.

APPENDIX 2

METHOD OF COMPUTING FORM RESISTANCE

Figure 63 represents a plane $C\,F\,D\,A$ normal to the surface of the model and intersecting it on the line $\overline{FD}$ through an experimental position G. P is the pressure difference at G due to the speed of the model.

θ is the angle between the surface of the model at G and the centerline of the model.

Figure 64 represents part of the body plan of the model showing the intercept of the plane through $\overline{FD}$ and the experimental position G.

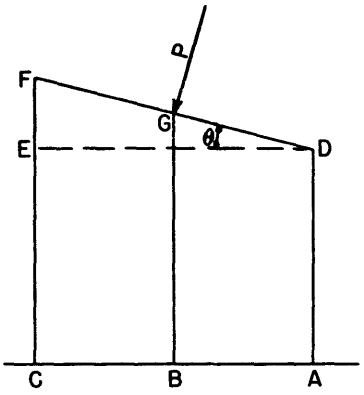

Figure 63

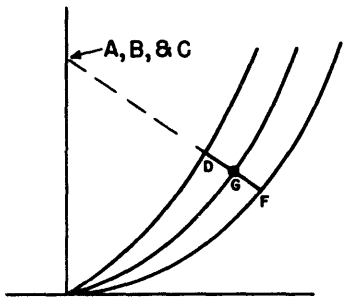

Figure 64

Pressure Area Diagrams

These figures illustrate the method by which the form resistance was computed.

The force producing the form resistance in the vicinity of the position G is the product of the pressure P multiplied by the area on which it acts, and resolved along a line parallel to the axis of the model.

$$Force = P(A \sin\theta)$$

where A equals area acted upon. Hence

$$R_{Form} = \int_{Stern}^{Bow} P(A \sin\theta)$$

Now $(A \sin\theta)$ is the projection of A on an athwartship plane, so the midship section of the model is the summation of $(A \sin\theta)$. Hence, if the various values of P are found and multiplied by the areas on the body plan to which they apply, the summation of these products will be the form resistance.

In this manner the variations of pressure over the body plan were plotted and contours of pressure were drawn.

Each area between adjacent contours was multiplied by the average pressure acting upon it. The algebraic sum of the products was the form resistance.